PROTON TRANSFER STUDY OF LOW-LYING STATES OF ^{136}La

PROTON TRANSFER STUDY OF LOW-LYING STATES OF ^{136}La

by

ARIF HASAN KHAN, B.Sc., M.Sc.

A Thesis
Submitted to the School of Graduate Studies
in Partial Fulfilment of the Requirements
for the Degree

Master of Science

McMaster University

September 1977

MASTER OF SCIENCE (1977) McMASTER UNIVERSITY

(Physics) Hamilton, Ontario.

TITLE: Proton Transfer Study of Low-Lying States of ^{136}La

AUTHOR: Arif Hasan Khan

SUPERVISOR: Professor R. G. Summers-Gill

NUMBER OF PAGES: ix, 57

ABSTRACT

The techniques of charged particle spectroscopy were utilized in studying the low-lying states of ^{136}La. Two proton transfer reactions were carried out on isotopically enriched targets of ^{135}Ba. Sixty-four energy levels of ^{136}La were observed up to an excitation of 1.8 MeV from $^{135}Ba(^{3}He,d)^{136}La$ and $^{135}Ba(\alpha,t)^{136}La$ reactions. Two methods were used to determine the ℓ-values for some of the states whose cross-sections could easily be obtained. One of the methods was to utilize the ratio of $(^{3}He,d)$ and (α,t) cross-section as an indicator of ℓ-values. The ℓ-values were also obtained from the angular distribution of the cross-sections of some of the multiplets.

The fore hand knowledge of the spin of the ground state made it possible to immediately assign spins to the first two excited states. Spins have also been assigned tentatively to a few other states using the 2J+1 rule.

In the process of this work, the relative Q-values for the $^{134}Ba(\alpha,t)^{135}La$, $^{135}Ba(\alpha,t)^{136}La$ and $^{136}Ba(\alpha,t)^{137}La$ reactions were also measured. The results show that the presently accepted proton separation energies for these lanthanum isotopes are considerably in error.

ACKNOWLEDGEMENTS

I would like to thank my supervisor, Professor R. G. Summers-Gill for his help in correcting and improving this thesis.

My thanks are also due to Dr. D. Burke for his guidance and fruitful discussions.

I am indebted to the past and present members of the group for assistance during long hours of experiments. I would especially like to thank Kevin LeNestour for his invaluable help with the Enge experiments.

I am thankful to the technical staff of the accelerator laboratory, especially to Jim Stark, Henry Harms and Y. Peng for their extra help in the events of crises.

I would also like to thank Mrs. Edith Luker for counting the plates and Miss Juanne Haykin for making a special effort to complete the drawings in time.

Finally, I am very indebted to Mrs. Edna Williams for her painstaking work in typing this thesis.

This work would not have been completed without the grant from the National Research Council of Canada. Deep gratitude is expressed for the financial assistance received from McMaster University.

TO MY WIFE

TABLE OF CONTENTS

LIST OF FIGURES

LIST OF TABLES

Introduction

The microscopic models of nuclear structure assume that all the nuclei are composed of neutrons and protons, and the properties of the nuclei can only be understood in terms of the interactions between nucleons. To understand the nuclear structure one attempts to represent these inter-nucleon interactions by a potential. In spite of the intensive work done in the field of nuclear forces, almost nothing is known about the strength of the three-body or many-body components of nuclear forces except that they are weak.

Bethe (1953) estimated that in the previous 25 years, more man-hours of work had been devoted to the problem of nuclear force than to any other scientific problem in the history of mankind. Even until the early sixties much confusion and conflict existed in the nature of nuclear force.

Since then, considerable success has been achieved in obtaining an average potential on which a nuclear structure model can be based. One of the most popular models is called the shell model. The concept of the shell model has been borrowed from atomic physics and carried over into nuclear physics. At present this model has a phenomenal success in explaining and predicting a vast amount of nuclear data.

This work is a humble attempt in investigating certain aspects of the nucleus ^{136}La in the guiding light of the shell model. ^{136}La has 57 protons and 79 neutrons. It is an odd-odd nucleus. Within the framework of the shell model one would attempt to study the interactions between the (Z-50) protons and (N-82) neutrons, i.e. 7 protons and 3 neutron holes. This is a rather complex system with a natural half-life of approximately 9 minutes. In spite of the fact that in the last decade or so, a considerable amount of work has been done on odd-odd nuclei in this mass region, no studies of ^{136}La have been made. Islam (1975) has studied the low-lying levels of ^{138}La and improved on

pre-existing experimental data of other researchers. The fundamental difference between the structures of the two nuclei is the number of the valence neutron holes. In the case of ^{138}La there is only one hole which can be in $2d_{3/2}$ and $3s_{1/2}$ orbits, whereas in ^{136}La there are three holes to be accommodated in the same most likely orbits. The nature of this interaction between these holes and the seven protons beyond the shell closure at 50 would be manifested in terms of the energy levels with definite spins and parities. It is expected that ^{136}La is a spherical nucleus and hence, the shell model can successfully describe the low-lying states in a relatively small configuration space.

The study of odd-odd nuclei is considerably more difficult than other nuclei. Experimentally, there are several reasons. Often the mass of a particular odd-odd nucleus is greater than that of both its neighbouring even-even isobars, which makes it impossible to observe levels in the odd-odd nucleus by γ-ray and β-ray spectroscopy of the radioactive decay. In situations where levels in an odd-odd nucleus can be populated by beta decay the daughter nucleus itself is often unstable; this demands stringent experimental techniques. Also, the decay occurs from zero spin and positive parity, therefore, only states with small spins will be observed!

The reaction spectroscopy lets us observe more states in odd-odd nuclei but in our mass region the density of levels is very high. Also, the resolution is much poorer than in gamma-ray studies.

The simple phenomenological models do not describe the low-energy spectra adequately. The nature of the neutron-proton residual interaction strongly affects the ordering of the levels in the multiplets which arise from a specific neutron and proton configuration. This very effect of the residual interaction makes the study of ^{136}La so important. The detailed level structure gives the

information about the interaction.

In this present work the charged particle spectroscopy technique was used to get the information about the low-lying levels. The proton transfer reactions were carried out using ^{3}He and α beams of 24 and 27 MeV, respectively, on ^{135}Ba targets. The ground state spin and parity of the target nucleus is $3/2^{+}$ which is due to the neutron hole in the $2d_{3/2}$ orbit. The proton in $^{135}Ba(^{3}He,d)^{136}La$ and $^{135}Ba(\alpha,t)^{136}La$ reactions, can be transferred to the $2d_{5/2}$ or $1g_{7/2}$ state. The shell model systematics of the neighbouring nuclei suggest that the low-lying states of ^{136}La would be due to the coupling of the neutron hole in $2d_{3/2}$ or $3s_{1/2}$ to the transferred proton in $2d_{5/2}$ or $1g_{7/2}$. At higher excitations the group of negative parity states arising from the coupling of the $d_{3/2}$ neutron hole to a proton in $h_{11/2}$ have been identified. The first negative parity state in ^{136}La was found to be at an excitation of 1005 keV which is the same location of state in ^{137}La. Further comparisons with other neighbouring nuclei would indicate that ^{136}La does conform to the norms of shell models.

Chapter I contains the theoretical background pertinent to the clear comprehension of the present work. The main purpose of Chapter I was not only to discuss basic theory, but also to show the underlying approximations and assumptions which are crucial to the interpretation of the results. In Chapter II the details of experimental technique and the results are presented. Interpretation follows in Chapter III.

Chapter I

THEORETICAL PRELIMINARIES IN NUCLEAR PHYSICS

I.1 A Brief Historical Sketch

The studies in so-called modern Physics started very late in the nineteenth century. The discovery of continuous x-rays by Roentgen, 1895, created extreme interest among the physicists and prepared the ground for Becquerel's observation in 1896 of the radio-activity of uranium. Within a year the electron was identified as a fundamental particle by J.J. Thomson, followed by the discovery of polonium and radium as new radioactive elements by Pierre and Marie Curie. At the turn of the century two important events took place: Ernest Rutherford observed the exponential decay of thoron gas and Max Planck put forward his quantum hypothesis. In 1903 Rutherford and Soddy proposed the transformation theory of alpha- and beta-decay.

In 1908 Rutherford and Geiger were able to measure the charge of the α-particle to be twice that of the electron and the following year Rutherford and Royds identified it to be a helium ion by detecting the helium gas evolved from radon. Marsden and Geiger carried out α-particle scattering experiments of paramount importance, which led Rutherford to postulate the nuclear atom in 1911. Neils Bohr worked out the theory of the nuclear-atom model which solved many problems in atomic spectroscopy. In the same year i.e. 1913, Moseley derived the atomic numbers Z from the characteristic x-ray spectra. In 1914 Rutherford and Robinson found the mass of α-particle to be four times the proton mass.

In later years Rutherford, Marsden and others observed the first nuclear reaction initiated by α-particle. Within these twenty-five years so many

experimental discoveries were made, that obviously the next phase was the era of great theoretical advancement consolidated by the experimentalists. De Broglie proposed the theory of matter waves in 1924; two years later Schrödinger evolved his wave equation. In 1927 Germer, Davisson and G.P. Thompson observed the diffraction of electrons. In the same year Heisenberg proposed his celebrated unbestimmtheits prinzip. The following year Gamow, Gurney and Condon published the Theory of Potential Barrier Penetration, the fact that quantum mechanics allowed a barrier to be penetrated led to a phase of remarkable progress in devising artificial means of accelerating sub-atomic particles. The cyclotron of Lawrence and the electrostatic accelerator of Van de Graaff were devised in 1932. In the same year, two very important events took place; Cockroft and Walton observed the first artificially induced nuclear reaction and Chadwick identified the neutron. Tremendous technological development took place which made vacuum pumps, electronic counters and new and sophisticated detecting devices available.

I.2 Shell Model and Nuclear Structure

For atoms a planetary picture existed e.g. our solar system, with the sun being the center or one of the focii of the circular or elliptical orbits of the planets revolving around it. The idea of nuclear matter was realized by Heisenberg and Majorana in their first papers of nuclear structure. In 1933, Majorana says: "One finds at the center of the atom a sort of matter which has the same property of uniform density as ordinary matter."

The most significant and fascinating property of finite nuclei is the fact that their radii are proportional to the cube root of their masses:

$R = r_o A^{1/3}$, r_o being the constant of proportionality. Probably this relation was suggested by Gamow!

The first neutron-proton nuclear model was proposed by Iwanenko and Heisenberg. In 1932 Bartlett made the first suggestion of neutron-proton shell structure analogous to the electron shells of the atoms and two years later Gamow (1934) observed that the plot of (A-Z)/Z against A for stable nuclei has the form of a band with a somewhat irregular periodicity and suggested a correlation between the windings and a possible shell structure. Magic numbers Z=50, 82 and 126 were observed by Elsasser (1934). He published a paper and showed that these numbers can be correlated with closed shells in a model of non-interacting nucleons occupying the energy levels generated by a potential well with a central elevation called wine-bottle potential.

The concept of shell structure was overshadowed by the concomitant development of important ideas on charge-independent nuclear forces. However, in many calculations nuclear wave functions constructed from determinants of single-particle orbitals were used which suggested the admittance of shell structure. These calculations and experimental evidence suggested the inclusion of Z and N=2, 8 and 20 among the magic numbers.

Breit, Inglis and Dancoff, and Furry attempted to include spin-orbit coupling in the then-existing shell model. In the same period another remarkable and simple approach to nuclear structure was developed from the possibility of considering the α-particle as a unit in the structure of light nuclides such as ^{4}He, ^{12}C, ^{16}O, etc.

The idea of a compund nucleus (proposed by N. Bohr) and resonance formalism had overwhelming success in the field of nuclear reactions. As an unfortunate consequence the relevant work on shell structure practically

stopped. For a decade or so the shell model fell into oblivion. Then after World War II a review by Mayer (1949) revived the interest in shell structure. In 1949, the magic numbers were explained independently in terms of single-particle orbits by Mayer (1949) and Jensen (1949). The crucial point was the inclusion of spin-orbit forces which are essential for an understanding of the closed shells at magic numbers 50, 82 and 126.

Obviously, to understand the structure of complex nuclei one must resort to approximations, such as to assume that from the standpoint of any nucleon, the forces exerted on it by all the other nucleons in the nucleus can be represented by a potential well or shell theory potential. There were some conceptual problems in accepting the fact that nucleons travel in orbits without colliding with each other in spite of the existence of strong forces acting between them. Brueckner and collaborators succeeded in developing approximate solutions to the many-body problem. The explanation can only be due to the fact that a nucleus is not a classical system where numerous nucleons confined to such a small space moving with high velocity would have endless numbers of collisions. But it is a quantum system in which the nucleons are restricted to a very few allowed orbits. The further restriction from the Pauli exclusion principle severely limits the possibilities for collisions.

In a nuclear shell model attempts are made to explain shell closure property and predict electromagnetic and nuclear groud-state properties of the nucleus in terms of the uncorrelated motion of simple particles in the given mean potential.

As mentioned earlier to explain the magic numbers 28, 50, 82 and 126, a spin-orbit potential is added to the centrally symmetric potential which causes the splitting of $j = \ell \pm 1/2$ levels. With the introduction of the

the spin-orbit force, the model has been very successful in predicting the ground state spins of a large number of odd-A nuclei. Pauli's exclusion principle dictates that each orbit can contain a maximum number of $2j + 1$ protons and $2j + 1$ neutrons each with a different m quantum number. Each pair of like nucleons couple their j-values to give a total of zero i.e. the angular momentum is determined by the last unpaired nucleon. An evident consequence is that all even-even nuclei should have ground state spin zero, which is indeed the case. The shell model is not equipped to make predictions concerning the odd-odd nuclei since the model does not describe how the last neutron and the proton couple their j's. This extreme single particle model cannot be truly realistic, but it does lead to the conclusion that a closed shell forms an inert core and the properties of a nucleus are attributed to the extra-core nucleons. An equivalent situation exists when, instead of a nucleon beyond a closed shell, there is a hole, i.e. a deficiency of a nucleon in a closed shell. Racah (1942) studied the hole-nucleon interaction by utilising the techniques of tensor algebra. Pandya (1956) used an alternate approach for the jj-coupling case which is based on the property that the coefficients of fractional parentage connecting the states of one- and two-hole systems have a particularly simple analytical form. From this approach the energy levels of a particle-hole system can directly be obtained in terms of the energy levels of the corresponding particle-particle system. This theorem can be applied to any pairs of odd-odd nuclei consisting of nucleon-nucleon and nucleon-hole systems as long as the validity of the j-j coupling is reasonably assured and experimental values of the energy levels are available.

The understanding of the structure of nuclei includes all aspects of the dynamics of intra-nuclear nucleons: the energies binding them to each

other, the Coulomb forces (in cases of protons), their momenta and the correlation between them. The true total wave function of the nucleus contains the complete description of nuclear structure. But it would be a formidable task to determine the behaviour of all the degrees of freedom of a dynamical system such as a moderately heavy nucleus. Therefore, one must resort to approximations and assumptions. One of the assumptions is that the many-body interactions are relatively weak and only two-body interactions are important. It gives rise to the reduced Hamiltonian of the system, consisting of the kinetic energy operator and the inter-nucleon potential V_{ij} which in turn is used to calculate the wave-functions for each nucleon. The many-body eigenfunctions are represented by the anti-symmetrized product of single particle wave-functions of the Hartree-Fock potential. The Hartree-Fock method is a systematic method of seeking approximate solutions to the many-body problem. As far as the nucleus is concerned the nature of two-body interactions is such that even with the rather drastic assumptions underlying the HF method, the problem is still very difficult. Therefore, further approximations are made and various types of HF calculations are being carried out by different groups. The self-consistent symmetries of the HF solution are such that if once they are present at any stage of interaction they remain so throughout all subsequent interactions. These symmetry properties can be imposed on the HF wave-function by introducing external constraints. A typical constraint is the inert core which is assumed to be invariant under the variations implicit in the HF method. If this is the case then the self-consistency problem need be solved only for the "loose" or extra-core nucleons.

The main justification of all assumptions is that they make the calculations very much easier and faster. But to obtain a better microscopic

agreement between the theory and the experiment one is forced to consider the presence of a suitable residual interaction between loose nucleons. The problem of many strongly interacting particles is very difficult and a simplified model is not expected to render a complete description of the nuclear phenomena. The use of a simple schematic interaction permits a simple and fruitful search for new phenomena in the nuclear structure and understanding of qualitative features of nuclear states, but no detailed quantitative description can be expected. There are more sophisticated theories where so many assumptions are made that it is impossible to make any predictions.

Green and Moszkowski (1965) introduced a very simple interaction - it is a generalization of a pairing force. The calculations of Brueckner and collaborators suggested that the pairing energy would be of the order of 100 keV in the nuclear matter. But the empirical pairing energies (1-2 MeV) are due to interactions at the nuclear surface. Therefore, they drew the conclusion that most of the interactions take place at the nuclear surface i.e. the nucleons move independently inside the nuclear interior and collide only when they are on the nuclear surface. The kind of agreement one obtains with experiment, at least in some cases, is of the same order as that which results when a much more realistic interaction is used (Hamada-Johnston) instead of the so-called surface delta interaction (SDI). Hence, it can be asserted that SDI contains some of the essential features of the shell-model calculations. Therefore, one is justified in using such a simple two-body interaction to study the shell-model techniques. This interaction is defined as

$$V_{SDI}(ij) = -4\pi A_T \, \delta(\Omega_{ij}) \, \delta(r_i - R) \, \delta(r_j - R)$$

where Ω_{ij} is the angular coordinate between the interacting particles i

and j and R is the nuclear radius. $A_T = A_0$ or A_1 for T=0 or T=1, where T=1 is the isospin state in which two protons or two neutrons can only interact, but a neutron-proton pair can be formed in both the isospin states, T=1 and T=0. Therefore, A_1 and A_0 are the only parameters that enter the expression of the two-body matrix elements.

The strengths A_1 and A_0 are determined, from shell-model calculations for the theoretical energies, in such a way that the best fit of the calculated energies to the empirical ones renders the suitable values for A_0 and A_1. The application of SDI met with considerable success in describing the properties of the odd-even and the even-even nuclei (Green and Moszkowski, 1965).

Glaudemans, Brussaard and Wildenthal (1967) modified the SDI by adding a T-dependent, but J-independent, term to the SDI potential

$$V_{ij} = - 4\pi A_T \delta(\Omega_{ij}) \delta(r_i-R) \delta(r_j-R) + B_T .$$

The term B_T is added to the diagonal matrix elements only and the two parameters B_1 and B_0 are independent of J but they affect the energy spacing between the groups of $T=T_1$ and $T=T_2$ states. The N=82 nuclei were extensively studied both experimentally and theoretically by Wildenthal (1969, 1971). Hussein (1973) showed that such an interaction can also give a good description of the odd-odd nucleus ^{142}Pr.

I.3 Nuclear Reactions

I.3a Compound Reactions

Although this work exclusively depends on the presumption that the reactions ^{135}Ba(^{3}He,d)^{136}La and ^{135}Ba(α,t)^{136}La are direct, it would be more than appropriate to take a look at the class of reactions called compound-nucleus reactions. This concept of nuclear reactions was presented by

Niels Bohr in 1936. A compound nucleus can be formed by bombarding a nucleus A with a "particle" a. The nucleus A and the particle a amalgamate to form the compound nucleus C^*. Since this is a system of strongly interacting particles the incident particle has a very short mean free path for interaction with other nucleons and, as a result, its energy is very quickly shared among all the other nucleons. The compound nucleus decays to the final product when sufficient energy is again associated with one particle so that it can emerge. If the initial kinetic energy of the incident particle is small this may take a very long time, therefore, the decay lifetime may be of the order of $\sim 10^{-14}$ sec., which is certainly very long compared to the traversal time of $\sim 10^{-21}$ sec.. Hence, it is assumed that the mode of decay of the compound nucleus is independent of its mode of formation, except for the requirements of the various conservation laws. In simple words once a compound nucleus is formed all the information regarding its formation is lost. The decay process can be treated statistically on the assumption that the probability of decay by the emission of different kinds of particles such as α, p, n, etc., is the same. The validity of Bohr's hypothesis of the compound nucleus has been confirmed by several experiments. One such experiment was performed by Ghoshal (1950) in which he produced the same compound nucleus $^{64}Zn^*$ with the bombardment of $^{60}_{28}Ni$ by α particles and $^{63}_{29}Cu$ by protons.

If the energy of the incident particle is relatively low, the spacings of the levels are greater than the widths of the levels excited; consequently the decay of the level will take place from a well-defined state of the compound nucleus i.e. the reaction is essentially an isolated resonance process. In the case of higher energies the excited levels may overlap and the lifetime of the compound nucleus may be comparable

with the traversal time of $\sim 10^{-21}$ sec., hence, a departure from the compound nucleus behaviour is expected!

I.3b Direct Reactions

The class of reactions which includes inelastic nuclear collisions, stripping, and its inverse, the pick-up reaction, is called direct reactions. A direct reaction proceeds without the formation of a compound nucleus, because the time during which the incident and target nuclei interact is very much shorter than the life of a corresponding compound nucleus. At low energies, the compound-nucleus reaction is more favoured, whereas at higher energies, the direct reaction mechanism will prevail.

The direct reactions are ideally suited to studying low-lying excited states that are characterized by simple elementary excitations. Usually there is a very specific connection between a given type of level and the direct reaction by which it is strongly populated.

In most of the direct reactions it is possible to write a differential reaction cross-section as a product of two factors,

$$\frac{d\sigma}{d\Omega} = S\ \sigma\ (\theta)$$

where S determines the absolute magnitude of the cross-section, while $\sigma\ (\theta)$ describes the shape of the angular distribution as a function of scattering angle θ. The shape function is not very sensitive to the details of nuclear structure but the magnitude factor contains the structure information about the initial and final states. Hence, the magnitude factor S is called the spectroscopic factor. The structure information is extracted from absolute differential cross-section measurements by calculating the angular distribution $\sigma(\theta)$ in a suitable approximation and then the factor S is determined by normalization to the experimental

data and compared with values calculated from appropriate nuclear models.

We will only consider the direct reactions of the type A(a,b)B with two nuclei in the initial state and two nuclei in the final state. Also we will consider only one-particle transfer reactions in which the particles a and b differ by one nucleon. If a is heavier than b then it is a stripping reaction. If b is heavier than a then it is a pick-up reaction.

I.3c The Distorted-Wave Born Approximation

The most widely used suitable approximation is the distorted-wave Born approximation (DWBA). The DWBA treats the incident and emitted particles as moving under the influence of the long range Coulomb and short range nuclear force. DWBA assumes that elastic scattering is the major component of the reaction process and reactions may be treated by utilizing the well-known techniques of perturbation theory. Among many others, Satchler (1964, 1965) has given a lucid and profound explanation of the underlying mechanisms of DWBA.

The elastic scattering is realized in terms of a phenomenological two body potential, the so-called optical potential. The optical potential parameters are obtained from fitting the experimental data of elastic scattering experiments.

A DWBA calculation invqlves the matrix elements which contain the elastic scattering wave functions generated by the optical potentials. These calculations are extensive and can only be done with computers, but the result is a detailed prediction of the cross-section as a function of angle. Sometimes a zero-range approximation assumes that the outgoing particle is ejected from the same point where the incident particle is

absorbed. From the DWBA calculations it can be determined that the reactions occur in the region of r≈8 fermi although there are contributions from a wide range of radii. These calculations give not only the angular distributions but also the absolute cross-sections, $(\frac{d\sigma}{d\Omega})^{DWBA}$, under the assumption that during and after the reaction the changes in the nuclear structure follow some simple model. In general the model is that the transferred particle enters one of the orbitals without otherwise disturbing the nucleus. That is why it was possible to write the differential cross-section as a product of the spectroscopic factor S and the theoretical cross-section $(\frac{d\sigma}{d\Omega})^{DWBA}$, in the last sub-section:

$$\frac{d\sigma}{d\Omega} = S \left(\frac{d\sigma}{d\Omega}\right)^{DWBA}.$$

In stripping, a particle can be transferred into the nℓj shell of the target nucleus to form the residual nucleus - then the observed differential cross-section is related to the DWBA cross-section by

$$\left(\frac{d\sigma}{d\Omega}\right)^{exp}_{n\ell j} = \frac{N}{2j+1} \left(\frac{d\sigma}{d\Omega}\right)^{DWBA}_{n\ell j} C_T^2 \left[\frac{2J_B+1}{2J_A+1} \sum_j S_{n\ell j}(J_B) \right] .$$

where N is the normalization constant and depends on the type of reaction, C_T^2 accounts for the isospin coupling and J_A and J_B are the spins of the target and final residual nuclei, respectively. The angular momenta J_A and J_B are related to each other through the spin of the transferred particle obeying the vector-sum rule:

$$|J_A - j| \leq J_B \leq J_A + j$$

where $j = \ell \pm 1/2$. The sum rule often helps in ascertaining the single particle aspects of the final states in the residual nucleus.

The spectroscopic strength is denoted by $\frac{(2J_B+1)}{(2J_A+1)} S_{n\ell j}(J_B)$. The factor $(2J_B+1)$, called amplitude factor, appears in theoretical calculations and

in general it is not known. In fact it is one of the objectives of stripping-reactions studies to determine J_B.

The quantity $\frac{1}{2j+1}\left(\frac{d\sigma}{d\Omega}\right)^{DWBA}_{n\ell j}$ has been taken out of the summation, because it counts the cross-section per magnetic substate. The angular distributions for $\left(\frac{d\sigma}{d\Omega}\right)^{DWBA}$ peak in a relatively more forward direction for lower ℓ-values. This can be clearly seen from fig. II:2. The shapes of the angular distributions are characteristic of the ℓ-value of the transferred nucleon, whereas the j dependence is relatively small. In odd-odd nuclei, a state of given J_B may be populated by more than one ℓ-value. For example, in the $^{135}Ba(^3He,d)^{136}La$ and $^{135}Ba(\alpha,t)^{136}La$ reactions the proton states can be populated by $\ell_p = 0 + 2$ or $\ell_p = 2 + 4$ or even $\ell_p = 0 + 2 + 4$. In such a case the shape and magnitude of the differential cross-sections are quite different. One would attempt to determine the degree of admixture, if it is possible at all.

The DWBA calculations for $^{135}Ba(^3He,d)^{136}La$ and $^{135}Ba(\alpha,t)^{136}La$ show yet another interesting feature - the cross-sections for $(^3He,d)$ reaction increase with the increasing excitation energy while for (α,t) they decrease. See fig. II.5. This very feature and the fact that different ℓ-values are favoured in the above reactions offer an alternative method of obtaining ℓ-values. For example, the ratio of the cross-sections for the above reactions depends on the appropriate ℓ-values and the excitation energies and is independent of the spectroscopic strength and the target spin. By comparing the experimental ratio for a given level with those computed for different ℓ-values, one can obtain the ℓ-value for that level.

It is difficult to estimate how good the basic DWBA assumption is. However, the use of DWBA calculations has developed into an extensive and highly sophisticated technology.

Chapter II

PROTON TRANSFER EXPERIMENTS

Introduction

In the framework of the nuclear shell model there is considerable evidence that systems of N=82 and Z=50 nucleons are tightly bound aggregates, and they form stable systems; in other words, both 82 and 50 are good closed shells. The properties of low-lying states of a system which has few extra particles or holes beyond the closed shells can be explained in terms of the configurations arising from the (Z-50) protons and (N-82) neutrons.

In the case of ^{136}La there are three neutron holes which are occupying the orbits $3s_{1/2}$, $2d_{3/2}$ and $1h_{11/2}$ and seven protons distributed over $2d_{5/2}$ and $1g_{7/2}$ orbits.

In the lowest seniority scheme, levels of ^{136}La should arise from the various possible couplings of the odd proton and the single neutron hole.

From j-j coupling scheme, where $|j_p - j_n| \leq J \leq j_p + j_n$ holds true, the spins of the low-lying levels can be obtained. Following are the positive parity levels:

$$(\pi 2d_{5/2}, \nu 2d_{3/2}^{-1}) \rightarrow 1^+, 2^+, 3^+, 4^+$$
$$(\pi 1g_{7/2}, \nu 2d_{3/2}^{-1}) \rightarrow 2^+, 3^+, 4^+, 5^+$$
$$(\pi 2d_{5/2}, \nu 3s_{1/2}^{-1}) \rightarrow 2^+, 3^+$$
$$(\pi 1g_{7/2}, \nu 3s_{1/2}^{-1}) \rightarrow 3^+, 4^+$$

The negative parity states involving the $1h_{11/2}$ orbit are:

$$(\pi 1h_{11/2}, \nu 2d_{3/2}^{-1}) \rightarrow 4^-, 5^-, 6^-, 7^-$$
$$(\pi 1h_{11/2}, \nu 3s_{1/2}^{-1}) \rightarrow 5^-, 6^-$$
$$(\pi 1g_{7/2}, \nu 1h_{11/2}^{-1}) \rightarrow 2^-, 3^-, 4^-, 5^-, 6^-, 7^-, 8^-, 9^-$$
$$(\pi 2d_{5/2}, \nu 1h_{11/2}^{-1}) \rightarrow 3^-, 4^-, 5^-, 6^-, 7^-, 8^-.$$

Since ^{135}Ba has a $d_{3/2}$ neutron hole in its ground state, the proton transfer experiments will readily populate the first two groups of positive parity levels. However, due to configuration mixing one could possibly see all twelve positive parity states involving the neutron hole in the $3s_{1/2}$ orbit as well.

The negative parity states due to $\pi 1h_{11/2}$ are expected to be found at higher excitations, and at even higher excitations one would expect to observe the proton states of $2d_{3/2}$ and $3s_{1/2}$ along with the neutron hole states $2d_{5/2}$ and $1g_{7/2}$.

To estimate the locations of proton states in ^{136}La, one is inclined to take a look at the odd lanthanum isotopes e.g. ^{139}La, ^{137}La and ^{135}La. The ground state of ^{139}La has $J^{\pi} = 7/2^+$, the first excited state ($\sim$166 keV) has $J^{\pi} = 5/2^+$ and the $\pi 1h_{1/2}$ state is located at 1420 keV. In the case of ^{137}La, the ground state has $J^{\pi} = 7/2^+$, first excited state ($\sim$10 keV) has $J^{\pi} = 5/2^+$ and the $\pi 1h_{11/2}$ state is located at 1005 keV. The trend continues - the ground state of ^{135}La has $J^{\pi} = 5/2^+$, the first excited state ($\sim$120 keV) has $J^{\pi} = 7/2^+$ and the $\pi 1h_{11/2}$ is located around 786 keV. As one considers the more neutron deficient lanthanum isotopes the energy levels get more compressed, but the interesting feature is the moving of the $7/2^+$ state towards higher excitations. From ^{139}La to ^{135}La this level, which is populated by $\ell_p=4$, has shifted approximately 285 keV with respect to the $5/2^+$ state populated by $\ell_p=2$.

The ground state of ^{138}La is populated by $\ell_p=4$ and the first four excited states are admixtures of $\ell_p=2$ and 4. This is quite according to the expectations. Now the interesting question arises about the ordering and locations of the states populated by $\ell_p=2$, 4, 5 in ^{136}La. The encouraging factor is the fact that the ground state of ^{136}La is populated by $\ell_p=2$.

From the above information one would expect the lowest-lying states of ^{136}La to be populated by $\ell_p=2$, the states populated by $\ell_p=4$ to lie around 160 keV

and the proton negative parity states to be located around 1000 keV.

Similarly, one can also obtain some knowledge about the location of the neutron hole state from the neighbouring odd-A (79 neutrons) nuclei i.e. ^{135}Ba and ^{137}Ce. In ^{135}Ba the neutron hole state ($1h^{-1}_{11/2}$) is located 268 keV, whereas in ^{137}Ce an isomeric state due to the ($1h^{-1}_{11/2}$) neutron is located at 254 keV. Hence, in ^{136}La one would expect the location of this state to be around 260 keV. Again, the $s^{-1}_{1/2}$ neutron states are located at 221 keV in ^{135}Ba and at 160 keV in ^{137}Ce. In ^{136}La one might find this state to be around 200 keV. See Table III.1 for a comparison of ^{136}La with its neighbouring odd-A nuclei.

It is unfortunate that no other single particle transfer reactions could also be carried out. In the neighbourhood of ^{136}La there is only one other stable isotope. This is ^{138}La, suitable for (p,t) reaction. However, it is less than 0.1% in natural isotopic abundance which makes the availability difficult and very costly.

A combination of (^{3}He,d) and (α,t) reactions provide a more profound understanding of the low-lying states. The (^{3}He,d) reaction was chosen for angular distribution purposes despite the fact that the resolution is not as good as in the (α,t) reaction: a typical resolution in the (^{3}He,d) reaction was 18 keV. There are two reasons for this choice (i) the (^{3}He,d) reaction cross-section is about 5 times larger than the (α,t) cross-section at 27 MeV, and (ii) the diffraction patterns for angular momentum transfers of ℓ=0, 2, 4 and 5 have prominent features.

There were three main reasons to perform the (α,t) reaction: (i) the outgoing triton has approximately half of the energy of the deuteron (from the (^{3}He,d) reaction), hence the resolution was much better in this reaction ($\sim$12 keV at the FWHM); (ii) to obtain values from the ratios of (^{3}He,d) to

(α,t) cross-sections, as the dependence of the cross-sections on ℓ is different in these reactions, and (iii) to measure the differences in Q-values for $^{134}Ba(\alpha,t)^{135}La$, $^{135}Ba(\alpha,t)^{136}La$ and $^{136}Ba(\alpha,t)^{137}La$.

These reactions will be discussed in some detail in the subsequent sub-sections.

II.1 Experimental Prerequisites and Procedures

An undertaking such as ours has certain definite requirements: there are not many nuclear physics research laboratories in the world where one can carry out experiments of this nature. Following are the most important requirements:

i) A well defined monoenergetic beam of projectiles of suitable energy and current.

ii) A target fulfilling the requirements of stability, enrichment and uniformity.

iii) An analyzing instrument assuring a maximum degree of resolution.

iv) A device to detect the scattered charged particles.

v) Reliable computer programs and large computers to facilitate the final analysis of data in a reasonable length of time.

I would like to briefly describe the facilities provided by the Physics Department of McMaster University.

II.1a The FN Tandem Van de Graaff

The FN Tandem Van de Graaff accelerator, rated at 7.5 million volts on the terminal, manufactured by High Voltage Engineering Corporation is a suitable machine for providing high energy projectiles. Thanks to the technical staff of the Tandem Accelerator Laboratory, the terminal voltage can be maintained at 9 million volts, which is highly desirable in some of

the reaction experiments.

An ion source produces negative ions e.g. H^-, D^-, $^3He^-$, $^4He^-$ etc. which are passed through a magnetic field to select the desired ions. These negative ions accelerate towards the high voltage terminal which is positive with respect to the ground and located inside a large tank which is pressurized by SF_6 gas, (the use of SF_6 gas is the main reason the McMaster Tandem can be operated at 9 million volts). At the terminal a thin carbon foil (a gas stripper is also used) strips a number of electrons from the negatively charged ions. Thus the ions experience a repelling electric force which provides more kinetic energy for them. The maximum energies one can get are proton and deuteron beams of 18 MeV and ^3He and ^4He beams of 27 MeV. They are focused through a set of object slits. An analyzing magnet selects the ions of right energy by deflecting them through 90^0. Part of the analyzed beam hits the image slits which being transmitted through it. A feedback system controls the stabilization of the terminal voltage. Then the beam is directed to the desired experimental set up by a switching magnet. A well focused beam on the target is highly desirable.

II.1b <u>The Target</u>

In our proton transfer experiments only barium targets were used. Oak Ridge National Laboratory provided the enriched barium isotopes in the form of nitrate. The isotopic enrichment of ^{135}Ba was more than 93%, see Table II.1. As most of the alkaline earths are quickly oxidized, it was necessary to use BaO as the target material. Hence $Ba(NO_3)_2$ was converted into BaO by heating it up to 800^0C. The BaO was heated under vacuum and evaporated on a thin(30 $\mu gm/cm^2$) carbon coating on a glass slide. These commercially prepared glass slides were treated with adenine and then

coated with carbon. Various thicknesses of BaO were deposited on the carbon, ranging from 30 to 50 $\mu gm/cm^2$. Later on, these carbon foils were floated on water and mounted on aluminum frames. During the whole procedure of target preparation one has to be careful to avoid contaminating the target. It is unfortunate that self-supporting targets of BaO could not be prepared as it would have improved the resolution and we would not have to worry about the impurity peaks due to ^{13}C in the α and t spectra.

II.1c The Split-pole Enge Spectrograph

This magnetic spectrograph is described in detail by Enge and Spencer (1967). The main features of the spectrograph are the following: split-poles are used to achieve two-directional focusing with minimum aberrations (particles are successively passed through two magnetic wedges giving four fringe fields which contribute to the vertical component of the force), a large solid angle of acceptance, second order focusing over large momentum range and a kinematic shift adjustment to compensate for the kinematic broadening (Enge 1958). The spectrograph can be rotated (with respect to the beam direction) over a wide range of angles.

II.1d Charged Particle Detecting Devices

In the focal plane of the Enge spectrograph there is provision for using position sensitive detectors, a proportional counter or photographic emulsion. In this work photographic plates were used exclusively; to date at the McMaster Laboratory this method of detection offers the best resolution. These photographic plates (supplied by Kodak) have a 50 micron thick emulsion. They are 25 cm long and 5 cm wide; the width enables one to have two exposures on the same plate. The charged particles, which arrive at 45° to the plane of the emulsion, leave tracks which are counted

Table II.1

Isotopic Composition of the Target Materials

	Abundance of Isotope %						
	^{130}Ba	^{132}Ba	^{134}Ba	^{135}Ba	^{136}Ba	^{137}Ba	^{138}Ba
^{134}Ba	---	---	81.4	3.71	2.18	2.36	10.3
^{135}Ba	---	---	0.36	93.6	1.61	0.87	3.56
^{138}Ba	---	---	---	---	---	0.20	99.80

Isotopes of less than 0.1% of abundance are not shown.

in 0.25 mm strips under a microscope.

II.1e Data Handling Analysis

In most of the experiments we used a PDP-9 computer on line to collect the data from a surface-barrier Si(Li) detector which monitored the elastically scattered particles from the target. The PDP-15 computer is used to obtain the areas under the elastic peaks and to get the specific reaction information from a program called Maggie. For the programs which required a much larger memory we used the CDC 6400 at the McMaster Computer Center.

Connected with this work two programs were used: the University of Colorado distorted-wave code DWUCK 4 written by Kunz (1969) and the program called SPECTR (O'Neil 1970). DWUCK 4 calculates the reaction (elastic and inelastic) cross-sections, using appropriate optical model parameters. SPECTR finds the centroids, hence the energy, of the peaks (which represent energy levels in the deuteron or triton spectra) and extracts the areas of the peaks after subtracting a specified background. It fits all the peaks of the spectrum with a standard shape and performs a non-linear least squares fit to a skewed gaussian function.

II.2 Experimental Procedure

All the experiments were carried out in the Enge spectrograph scattering chamber. The beam passes through the thin target and stops in a Faraday cup, depositing its charge. A current digitizer measures the charge and converts it into electronic pulses which can be registered on a scaler. In addition to the Faraday cup, a Si(Li) surface barrier detector was used at an angle of 30° subtending a solid angle of 0.08 msr.

The purpose of using the Si(Li) detector was to detect the elastically scattered particles and thus to normalize the spectra in determining the

absolute cross-section. A suitable spectrograph solid angle was chosen to be 1.3 msr; this was reduced to 0.026 msr for elastic exposures.

In the case of the Ba(^{3}He,d)La exposures the Kodak NTB-50 photographic plates were covered with 0.84 mm thick aluminum absorbers to stop the particles heavier than the deuterons. In the (α,t) exposures the aluminum absorber thickness was reduced to $\sim$0.1 mm to allow the tritons to reach the emulsion. All the elastic exposures were taken without any absorbers.

The absolute cross-sections were calculated in two different ways: (i) determining the area of the elastic peak from the Si(Li) monitor and (ii) taking short elastic exposures and relating them to the Faraday cup counts.

Using the first method the normalization constant K is defined to be

$$K = \left(\frac{d\sigma(\theta)}{d\Omega}\right)_E \times \left(\frac{\Delta\Omega_M}{\Delta\Omega_{sp}}\right) \times \frac{1}{N_E} \times \frac{1}{T.P.} \quad \text{(correction due to the impurities)}$$

where $\left(\frac{d\sigma(\theta)}{d\Omega}\right)_E$ is the differential cross-section for elastic scattering, $\left(\frac{\Delta\Omega_M}{\Delta\Omega_{sp}}\right)$ is the ratio of the solid angles subtended by the monitor and the spectrograph, N_E is the number of elastically scattered particles in the monitor and T.P. is the target isotopic abundance percentage. Also, since the monitor does not have very good resolution, it might count the elastically scattered particles from heavy impurities such as Ta, etc. from the evaporator. To overcome this difficulty, short elastic exposures were taken and related to the counts in the monitor. Hence,

$$K = \left(\frac{d\sigma(\theta)}{d\Omega}\right)_E \times \frac{\Delta\Omega_E}{\Delta\Omega_{sp}} \times \left(\frac{N_{mon}}{N_{sp}}\right)_{\text{short exp.}} \times \frac{1}{N_E} \times \frac{1}{T.P.}$$

where $\left(\frac{N_{mon}}{N_{sp}}\right)_{\text{short exp.}}$ is the ratio of the counts in the monitor and in the

spectrograph for the short exposure and $\frac{\Delta\Omega_E}{\Delta\Omega_{sp}}$ is the ratio of the solid angles in the two exposures. However, this correction was approximately 2%. Now the differential cross-section for the reaction is

$$\left(\frac{d\sigma(\theta)}{d\Omega}\right)_R = N_{sp} \times K$$

where N_{sp} is the number of the scattered particles detected by the spectrograph.

By the second method the differential cross-section is given by the following expression:

$$\left(\frac{d\sigma(\theta)}{d\Omega}\right)_R = \left(\frac{d\sigma(\theta)}{d\Omega}\right)_E \times \frac{N_{sp}}{N_E} \times \frac{\Delta\Omega_E}{\Delta\Omega_{sp}} \times \frac{(B.H.)_E}{(B.H.)_R} \times \frac{1}{T.P.}$$

where $\left(\frac{d\sigma(\theta)}{d\Omega}\right)_R$ and $\left(\frac{d\sigma(\theta)}{d\Omega}\right)_E$ have been defined earlier, N_{SP} and N_E are the counts in the spectrograph and in the elastic peak (exposure taken at 30°) $\frac{\Delta\Omega_E}{\Delta\Omega_{sp}}$ is the ratio of the solid angles in the two exposures; $\frac{(B.H.)_E}{(B.H.)_R}$ is the ratio of the Brookhaven (Faraday cup) counts in the two exposures and T.P. is the isotopic percentage of the target.

Both methods of normalization agreed with each other within 4%. In general the relative cross-sections at different angles should be accurate within 15%, but the absolute values determined by either of the methods may be in error by as much as 30%.

II.3 The $^{135}Ba(^3He,d)^{136}La$ Reaction

A beam of ^3He particles at 24 MeV was used to carry out the experiments. The beam current depended on the condition of the ion source, and at times the current was over 2 microamperes. The entrance slit to the scattering chamber was 1/2 mm in earlier experiments. Since that caused background problems, later on it was changed to 1 mm. Experiments were performed over

a range of angles from 7.5° to 60°. The forward angles were taken in steps of 2.5° angles due to the impurity peaks masking the low-lying states of the spectrum. The impurity peak at forward angles in the low-lying region, is due to the presence of ^{13}C which is only 1.11% of natural carbon. The $^{13}C(^{3}He,d)^{14}N$ reaction has a very large cross-section, therefore, even such a small quantity of ^{13}C produces large peaks. From 25° to 50° the exposures were taken in steps of 5°. It was noticed that the resolution at back angles was not as good as at, say, 25°. Therefore, the deuteron spectrum at 25° was chosen to be shown in figure II.1. The resolution in this spectrum is ∿15 keV, whereas, the typical resolution is ∿18 keV.

The spectra were analyzed up to the excitation energy of 1500 keV. It was practically impossible to go any further due to the high level density. However, it was possible to obtain the energies and cross-sections for seven prominent states beyond 1500 keV. Besides impurity peaks, we were able to pick out the ^{137}La and ^{139}La levels in our spectra.

From all the $(^{3}He,d)$ exposures, the excitation energies were obtained and average values were calculated. The energy of an excited state can vary from spectrum to spectrum, due to the variations in the resolution or poor statistics or not being able to obtain proper peak-shape parameters for the program SPECTR. It is known that the uncertainties in energy increase with the increasing distance on the plate. There are variations of 4 or 5 keV in some of the energies. See Table III.2.

II.4 The Angular Distributions

It has been mentioned earlier that the ℓ-values for some of the energy levels of ^{136}La were obtained by measuring the ratios of $(^{3}He,d)$ to (α,t) cross-sections. This method is discussed at the end of this chapter. Now, it would only be natural to determine the ℓ-values from the angular

Fig. II.1

Deuteron spectrum from $^{135}Ba(^{3}He,d)^{136}La$ reaction. Notice the high level density above 1 MeV excitation.

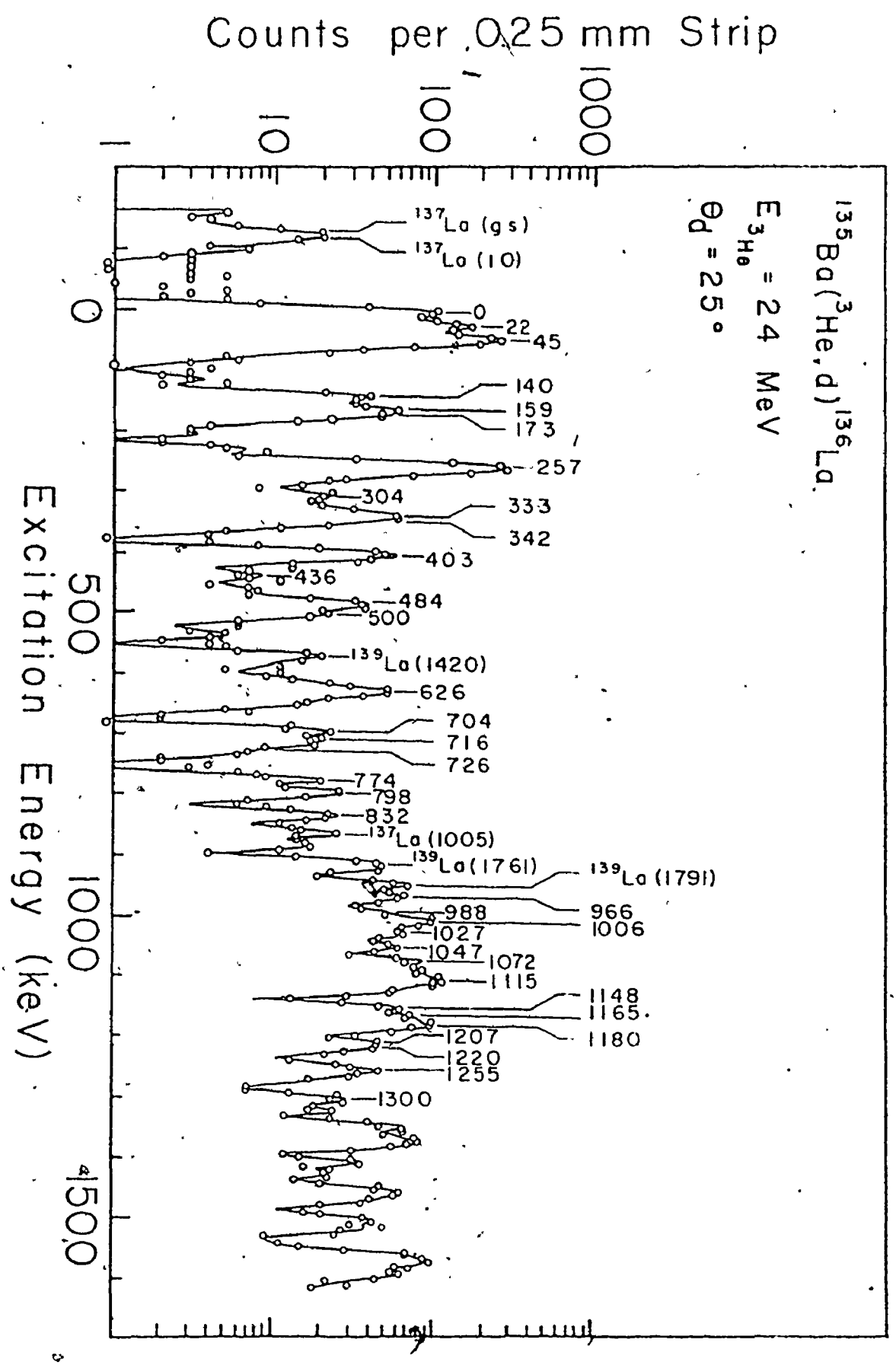
Counts per 0.25 mm Strip
1
10
100
1000
$^{135}Ba(^{3}He,d)^{136}La$
$E_{^{3}He} = 24$ MeV
$\theta_d = 25°$
^{137}La (g s)
^{137}La (10)
0
22
45
140
159
173
257
304
333
342
403
436
484
500
^{139}La(1420)
626
704
716
726
774
798
832
^{137}La (1005)
^{139}La(1761)
^{139}La (1791)
966
988
1006
1027
1047
1072
1115
1148
1165
1180
1207
1220
1255
1300
Excitation Energy (keV)
0
500
1000
1500

distributions and compare the results with the ratio technique. The angular distributions permit the evaluation of ℓ-values quite reliably.

As mentioned earlier, there are many levels in (^{3}He,d) spectra - over 90 levels up to the excitations of 1.6 MeV. Sometimes a specific peak has shoulders on both sides and from angle to angle the center of gravity changes considerably. Due to this high level density, it was possible to deduce angular distributions only for the multiplets. If these multiplets are populated by the same ℓ transfers then one should get better results due to better statistics. But if two levels are independently populated by totally different ℓ-values then the results would be erroneous.

The theoretical curves for ℓ= 0, 2, 4 and 5 for the reaction ^{135}Ba(^{3}He,d)^{136}La, were obtained from the DWBA calculations and shown in Fig. II.2. The optical model parameters are given in Table II.2 (Ishimatsu 1969). The experimentally determined results were best fitted to these curves. The angular distributions were plotted for the 12 states or groupings of states shown in Fig. II.3. The groupings are labelled with energies of the states which form the groups.

The angular distributions for the ground state and the first two show that these states are populated by ℓp=2. The next three states 140, 159 and 173 keV form a triplet whose angular distribution suggests that they may be populated by ℓp=4. It was necessary to plot the angular distribution for the triplet as a whole rather than individual states due to poor resolution and statistics. The angular distribution for the state at 257 keV strongly suggests that it is populated by ℓp=2. Similarly, the state at 403 keV seems to be populated by ℓp=2. The angular distributions for the state at 626 keV and the triplet, consisting of levels at 704, 716 and 726 keV, suggest that they may be populated by ℓp=2, but there could be admixtures of other ℓ-values. Some of the data points are missing at the forward angles; this is due to the presence of ^{13}C impurity peak. The angular distribution for the triplet which has a centre of gravity just

over 1000 keV suggests $\ell p=5$. Due to the high level density and relatively low cross-section for $\ell p=5$ in the (^{3}He,d) reaction, the angular distribution technique did not give satisfactory results for all the states populated by $\ell p=5$. The next set of data points for the triplet consisting of the energy states at 1072, 1115 and 1122 keV clearly shows that at least one of the states in the triplet is not populated by $\ell p=5$. The angular distributions for the next two triplets strongly suggest the presence of the states populated by $\ell p=0$. See Table III.2 for the ℓ-values which are determined through other means, as well.

II.5 The ^{135}Ba(α,t)^{136}La Reaction

It took a few attempts to collect reasonably good data for the (α,t) reactions. One is not always successful in getting a beam of 1-2 μamps for a considerable length of time from the McMaster University FN tandem Van de Graaff accelerator. This is the main reason that forced us to perform (^{3}He,d) reactions before the (α,t). However, (α,t) reactions were also carried out on enriched ^{134}Ba and ^{138}Ba targets.

The choice of the angles was very limited mainly due to ^{13}C impurity - only 50° was reasonably clean (up to 1.5 MeV). However, spectra were also taken at 35°, in spite of the impurity peak from 400 to 700 keV. Of course, this carbon peak was also present (at 35°) in the ^{134}Ba(α,t)^{135}La and ^{138}Ba(α,t)^{139}La reactions. The resolution was approximately 12 keV in the ^{135}Ba(α,t)^{136}La reaction. See Fig. II.4 for the triton spectrum taken at 50°. Also see Table III.2 for the energy levels observed in this reaction.

It is the characteristic of (α,t) reactions that the cross-sections for $\ell_p=0$, 2, 4, 5 transfers fall with excitation energy. For example at

Fig. II.2

The angular distributions calculated from DWBA for $^{135}Ba(^{3}He,d)^{136}La$.

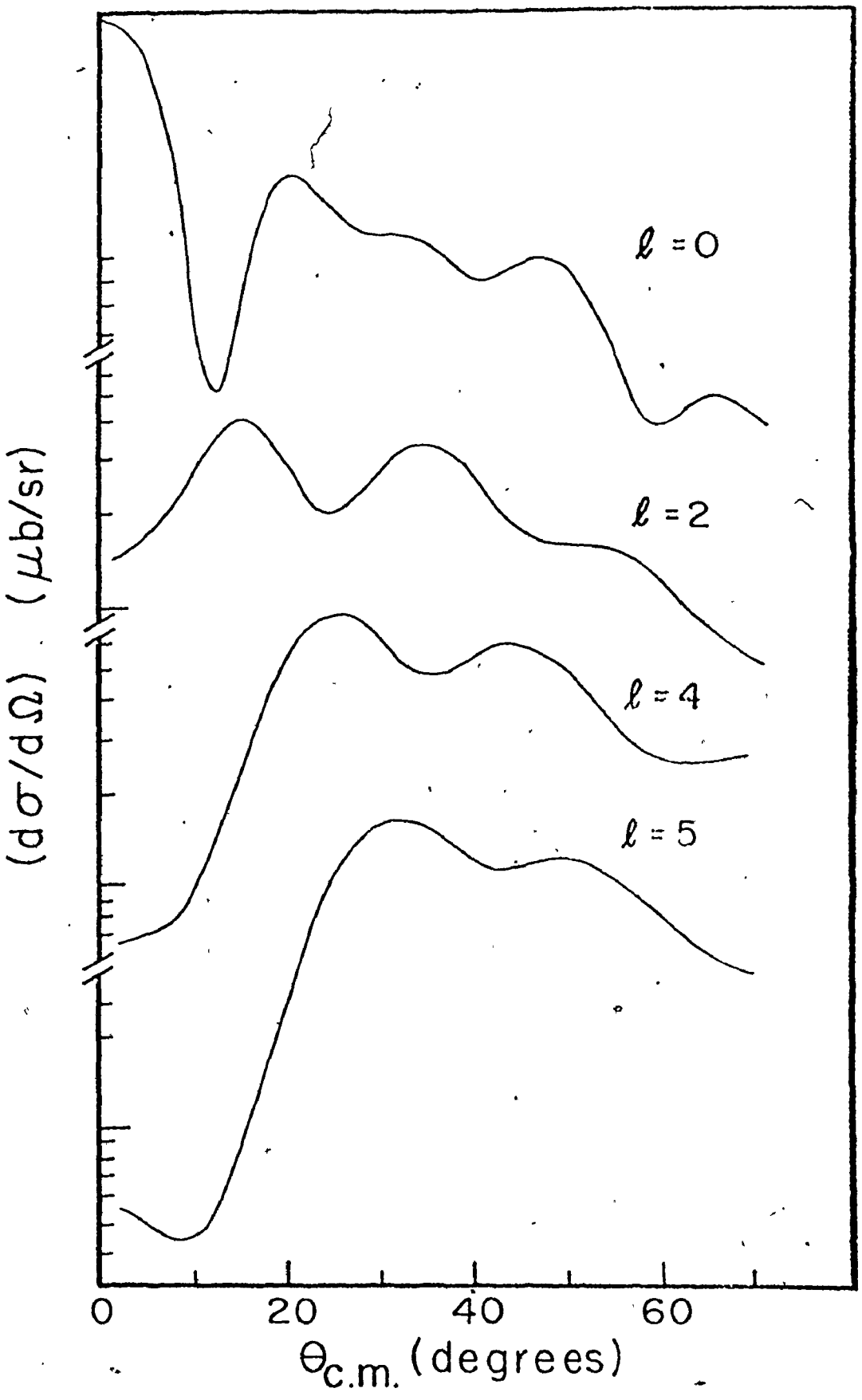
ℓ = 0
ℓ = 2
ℓ = 4
ℓ = 5
(dσ/dΩ) (μb/sr)
0
20
40
60
θc.m. (degrees)

Table II.2

Optical Model Parameters for the $^{135}Ba(^{3}He,d)^{136}La$ Reaction

Particle	V (MeV)	r_{oc} (fm)	r_o (fm)	a (fm)	W_S (MeV)	W_D (MeV)	r_o' (fm)	a' (fm)	V_{SO} factor	Non-local Correction Parameter
^{3}He	-172.0	1.40	1.14	0.70	-16.0	0	1.54	0.80	0	0.25
d	-101.4	1.30	1.085	0.857	0	61.0	1.29	0.788	0	0.54
p	*	1.20	1.20	0.65	0	0	0	0	8.0	0.85

$U(r) = U_C(r) + V(e^{x} + 1)^{-1} + iW_S(e^{x'} + 1)^{-1} + iW_D \frac{d}{dx'} (e^{x'} + 1)^{-1}$, where

$x = (r - r_o A^{1/3})/a$ and $x' = (r - r_o' A^{1/3})/a'$. $U_C(r)$ corresponds to the potential due to a uniformly charged sphere, radius $r_{oc} A^{1/3}$, charge $Z_A e$.

Finite range correction parameter = 0.770.

No radial cut-off was employed.

*Adjusted to reproduce separation energy.

Fig. II.3

Experimental deuteron angular distributions from the $^{135}Ba(^{3}He,d)^{136}La$. The solid curves are given by the DWBA calculations. They represent pure ℓ_p =0,2,4 and5 transfers best fitted to the data.

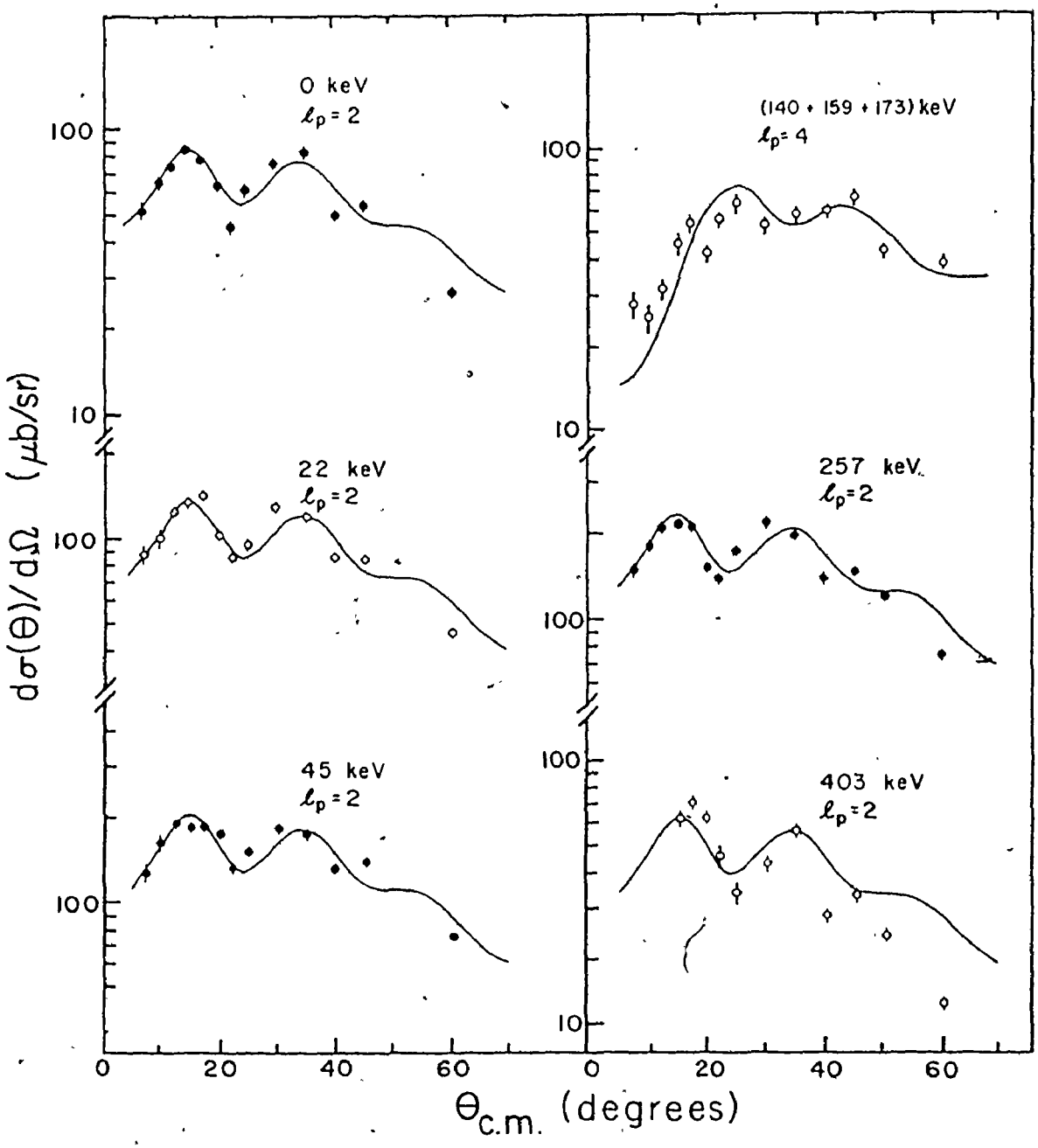
0 keV
$\ell_p = 2$
(140 + 159 + 173) keV
$\ell_p = 4$
22 keV
$\ell_p = 2$
257 keV
$\ell_p = 2$
45 keV
$\ell_p = 2$
403 keV
$\ell_p = 2$
100
10
0
20
40
60
$d\sigma(\Theta)/d\Omega$ (μb/sr)
$\Theta_{c.m.}$ (degrees)

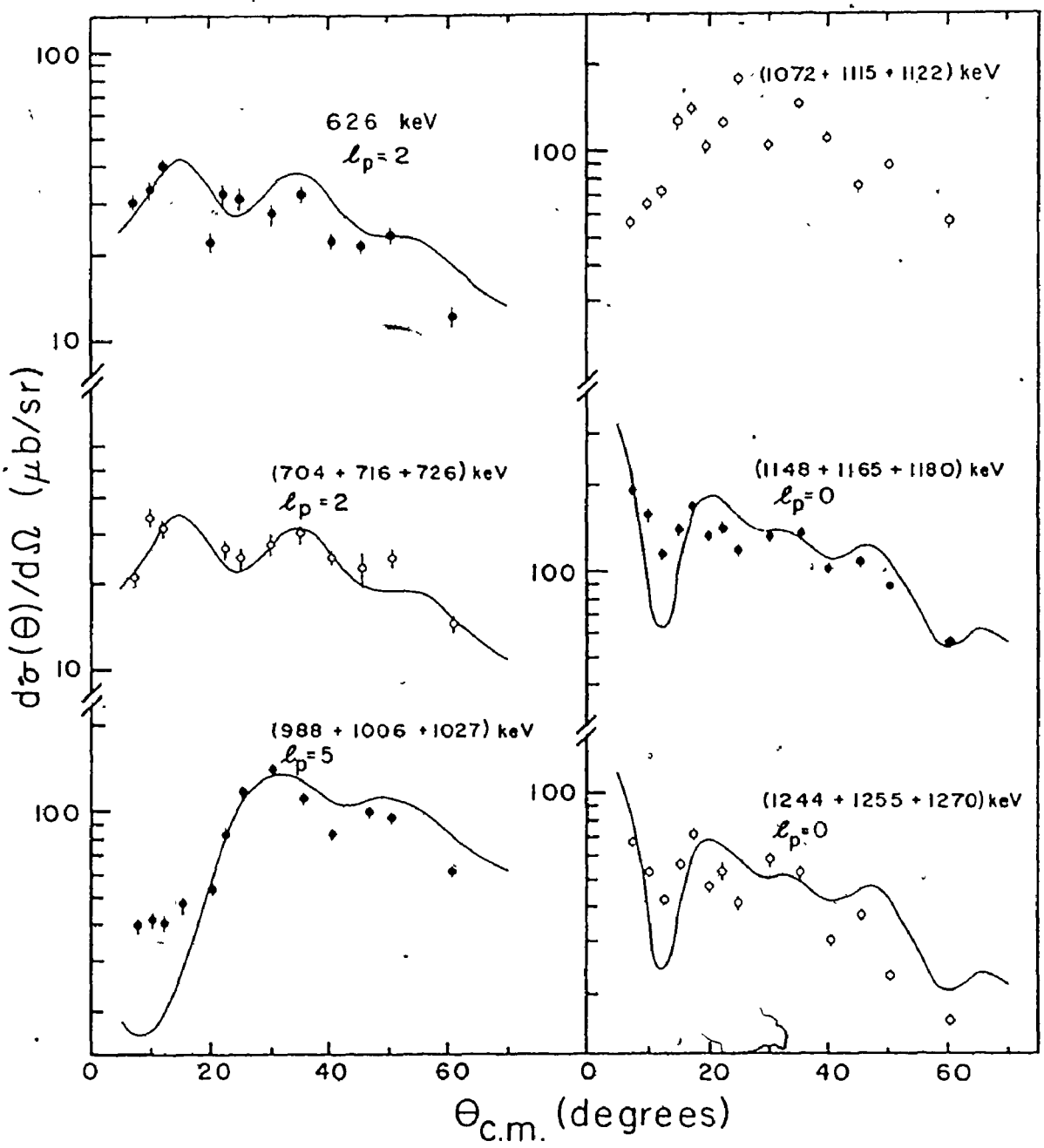
626 keV
$\ell_p = 2$
(704 + 716 + 726) keV
$\ell_p = 2$
(988 + 1006 + 1027) keV
$\ell_p = 5$
(1072 + 1115 + 1122) keV
(1148 + 1165 + 1180) keV
$\ell_p = 0$
(1244 + 1255 + 1270) keV
$\ell_p = 0$
100
10
0
20
40
60
$d\sigma(\Theta)/d\Omega$ (μb/sr)
$\Theta_{c.m.}$ (degrees)

Fig. II.4

The triton spectrum from $^{135}Ba(\alpha,t)^{136}La$ reaction.

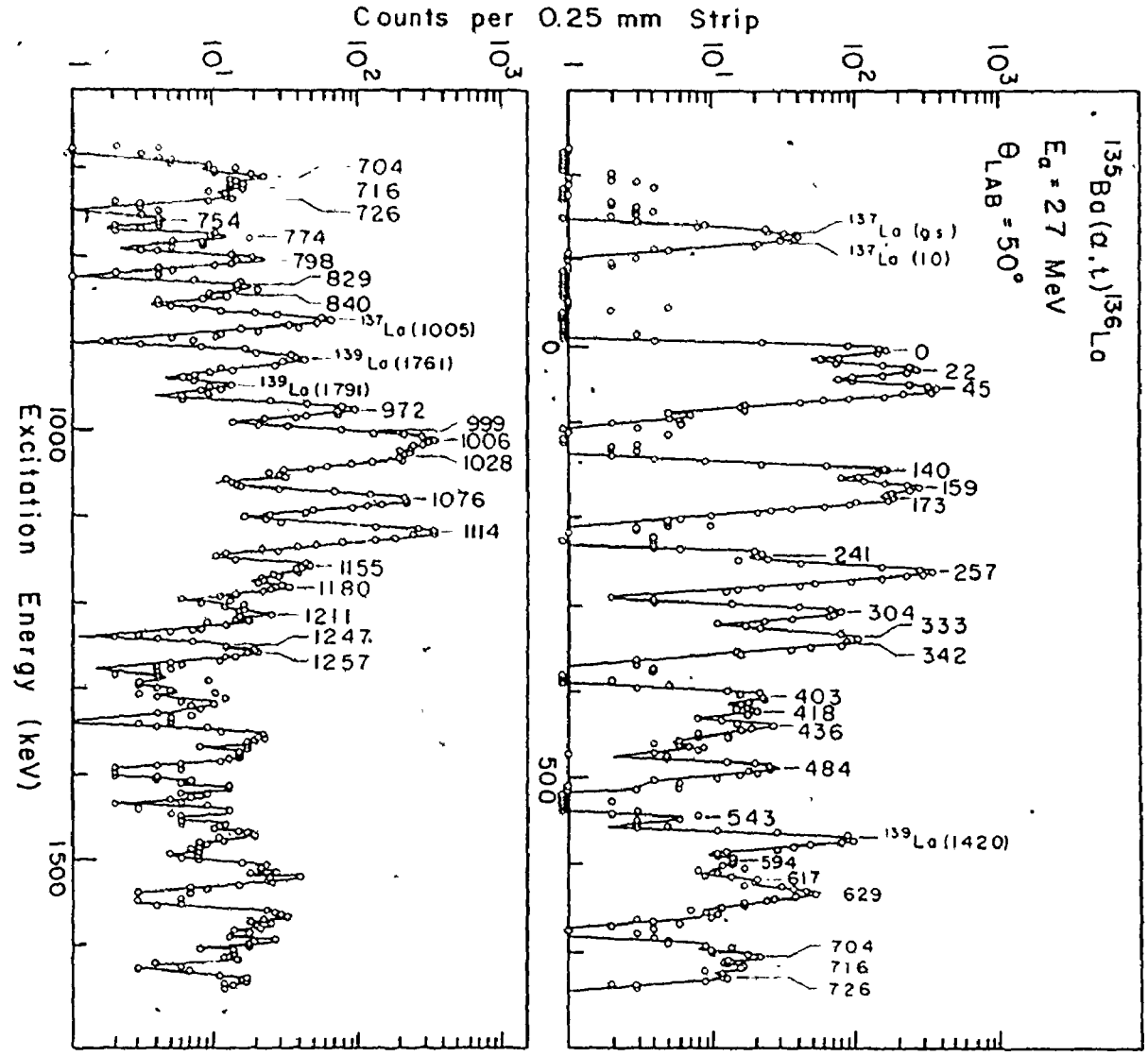
Counts per 0.25 mm Strip
Excitation Energy (keV)
$^{135}Ba(\alpha,t)^{136}La$
E_α = 27 MeV
θ_{LAB} = 50°
704
716
726
754
774
798
829
840
^{137}La (1005)
^{139}La (1761)
^{139}La (1791)
972
999
1006
1028
1076
1114
1155
1180
1211
1247
1257
^{137}La (g.s.)
^{137}La (10)
0
22
45
140
159
173
241
257
304
333
342
403
418
436
484
543
^{139}La (1420)
594
617
629
704
716
726

Fig. II.5

The theoretical cross-sections for $\theta_d = 45°$ and $\theta_t = 50°$ obtained from the DWBA calculations. The right hand side scale (1-10-100) is for the (α,t) reaction and the left hand side is for (^{3}He,d). Also the magnitude of the ℓ=0 curve for (α,t) is smaller by a factor of 10. The Q-value is for the (^{3}He,d) reaction.

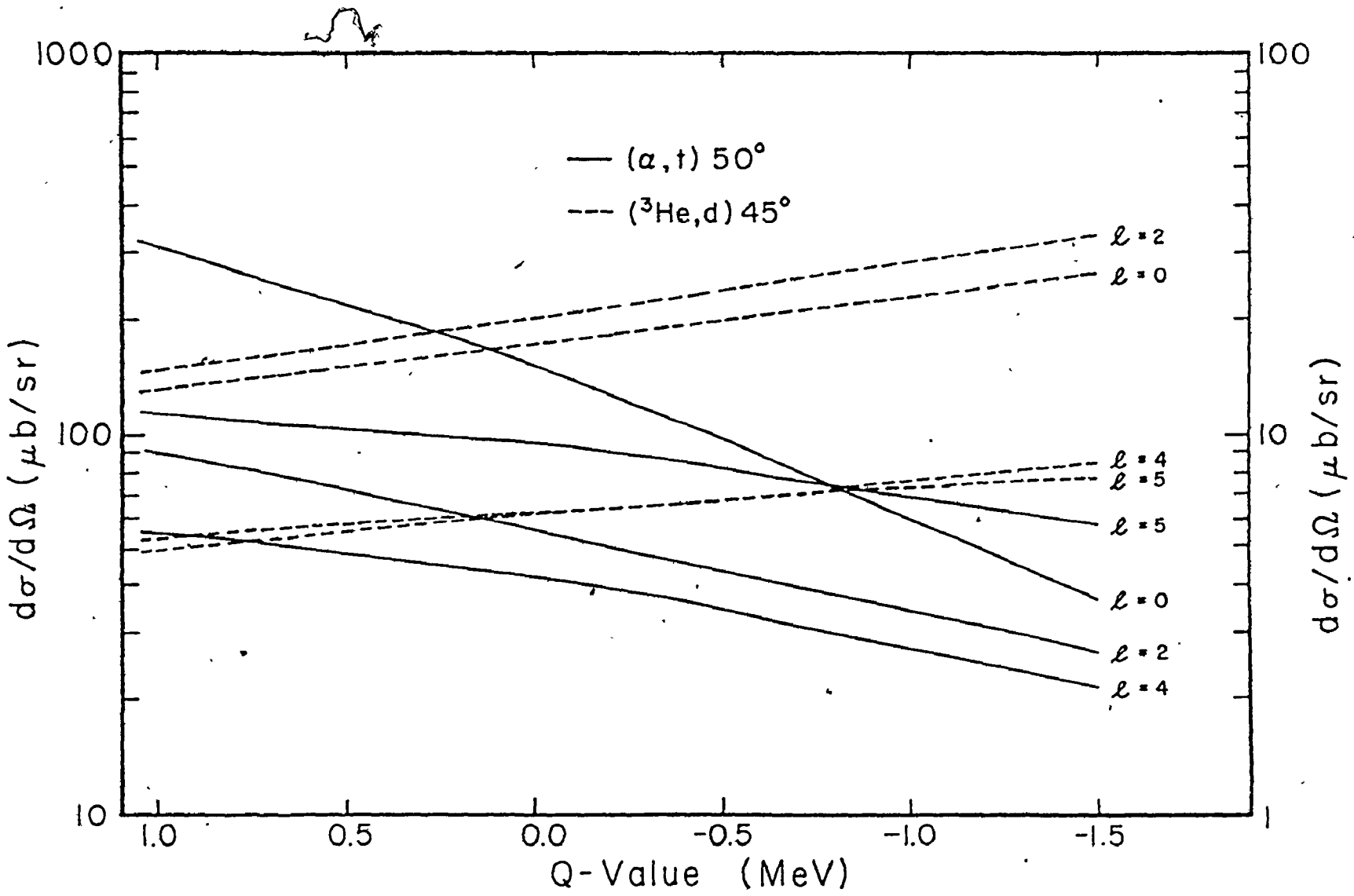
1000
100
10
100
10
1
— (α,t) 50°
--- (³He,d) 45°
ℓ = 2
ℓ = 0
ℓ = 4
ℓ = 5
ℓ = 5
ℓ = 0
ℓ = 2
ℓ = 4
dσ/dΩ (μb/sr)
dσ/dΩ (μb/sr)
1.0
0.5
0.0
-0.5
-1.0
-1.5
Q-Value (MeV)

Table II.3

Optical Model Parameters for the $^{135}Ba(\alpha,t)^{136}La$ Reaction

Particle i	V (MeV)	r_{oc} (fm)	r_o (fm)	a (fm)	W_S (MeV)	W_D (MeV)	r'_o (fm)	a' (fm)	V_{SO} factor	Non-local Correction Parameter
α	-200	1.30	1.40	0.60	-20		1.40	0.60	0	0.20
t	-200	1.30	1.40	0.60	-50		1.40	0.60	0	0.25
p	*	1.25	1.25	0.65	0	0	0	0	0	0.85

The expression for the potential is the same as that used for (^{3}He,d) reactions.

No radial cut-off or finite range correction was employed.

* Adjusted to reproduce separation energy.

excitation energy ∿1.7 MeV the cross-sections for ℓ_p=2, 4 and 5 fall by a factor of ∿2, whereas ℓ_p=0 cross-section falls by a factor of ∿5 (compared to the cross-sections at zero excitation energy). Consequently there are no states of considerable intensity, populated by ℓ_p=0 at higher excitation energies. Fig. II.5 clearly manifests the behaviour of (α,t) reactions.

In (^{3}He,d) reactions the trend is just the opposite i.e. the cross-sections for all ℓ transfers increase with the increasing excitation energy. We did not use the (α,t) reaction to get the angular distributions. There are two reasons for this:

(i) the Coulomb barrier for the outgoing triton is ∿10 MeV and the Q-value for the reaction is ∿-14.5 MeV, therefore, it was necessary to use particles of 27 MeV i.e. the tandem terminal voltage must be maintained at 9 million volts for very long periods, and,

(ii) the DWBA calculations show rather featureless angular distributions for (α,t) reactions at this energy.

II.6 Accurate Measurements of the Relative Q-values

During our work we observed the state of affairs of the Q-value of the following reactions: ^{134}Ba(α,t)^{135}La, ^{135}Ba(α,t)^{136}La and ^{136}Ba(α,t)^{137}La, as given in the Atomic and Nuclear Data Tables (Gove and Wapstra 1972).

Islam (1975) was the first one to determine the relative Q-value for ^{136}Ba(α,t)^{137}La which was known previously only from systematics. She measured the Q-value in terms of the known Q-value of ^{138}Ba(α,t)^{139}La and ^{137}Ba(α,t)^{138}La. All the masses of the stable barium isotopes have been measured by mass spectrometric methods. The mass of ^{138}La has been determined from the positron end-point energy in the decay of ^{138}La → ^{138}Ba

with an uncertainty of 14 keV. It should be possible to determine the nuclear masses accurately from nuclear reaction data.

According to H. Enge*: "At present, the masses measured by means of nuclear reaction data do not appear to be quite as accurate as the most exact mass spectrometer data. This is not because the method is inherently inferior, but because no concentrated effort has lately been exerted toward reducing these uncertainties significantly."

A target enriched in ^{134}Ba was used (see Table II.1 for the isotopic composition) and the exposure was taken at 35° for more than eight hours. The projectiles were α particles of 27 MeV and the current was ∿1.5 micro-amps. The nmr frequency was chosen to be such that the ground state of ^{139}La was focused at ∿6 cm from the edge of the photographic plate. The ground state of ^{137}La was around 10 cm on the plate and the ground state and the first excited state of ^{135}La were found to be in the middle of the plate immediately followed by the ∿1420 keV level of ^{139}La. With this arrangement it was just possible to get the 786 level of ^{135}La on the end of the plate. The peak areas and their respective energies were obtained from SPECTR. The counts in ^{139}La and ^{134}La peaks were more than 2,500, hence, the statistical error was minimized and the centroids of the peaks were obtained very accurately. The position of the ground state peak of ^{135}La was measured with respect to the ground state of ^{139}La and then with respect to the 1420 keV excited state.

Similar measurements were carried out at another angle, 50°, to ensure the reproducibility, and then the whole procedure was repeated to determine the relative Q-value for the reaction ^{136}Ba(α,t)^{137}La and the

* Introduction to Nuclear Physics, by H. Enge 1966. Addison-Wesley, p. 102

results were compared with Islam's measurements. Islam reported that difference in Q-values for the two reactions $^{138}Ba(\alpha,t)^{139}La$ and $^{136}Ba(\alpha,t)^{137}La$ to be 0.713 $\pm$ 0.003 MeV. Our result is 0.711 $\pm$ 0.003 MeV. The absolute Q-values measured in this manner would probably have an uncertainty of 15 keV, but the differences have uncertainties 3-4, keV. Burke and Balogh (1975) discuss the possible errors in detail.

The evaluation of the relative Q-value for $^{136}Ba(\alpha,t)^{137}La$ allowed the determination of the relative Q-value for the reaction, $^{135}Ba(\alpha,t)^{136}La$, as the ground state and excited states of ^{137}La and ^{139}La are present in all the spectra, see Fig. II.4, the result is -14.465 $\pm$ 0.015 MeV.

The Q-value for the reaction $^{138}Ba(\alpha,t)^{139}La$ is given by Gove and Wapstra (1972) to be -13.614 $\pm$ 0.014 MeV. From this value we have determined relative Q-values which have an uncertainty of 15 keV. Whenever the mass of ^{139}La is accurately measured, all these Q-values will be known. Until then they have an uncertainty of 15 keV.

Since the masses of the light nuclei are known with negligible uncertainty, one can obtain the Q-value for $(^3He,d)$ reaction if the Q-value of (α,t) reaction is known. The proton separation energies for ^{139}La are given by $S(P) = Q(\alpha,t) + 19815$ keV and

$$S(P) = Q(^3He,d) + 5494 \text{ keV}.$$

$$Q(\alpha,t) - Q(^3He,d) = 5494-19815 \text{ keV}$$

$$= -14321 \text{ keV}.$$

We received the latest issue of Atomic and Nuclear Data Tables Vol. 19, No. 3, 1977, with new Q-values, while this work was in the process of being completed. It was decided that the results from the present work should be compared with the most recent Q-values for the reactions. See Table II.4. In terms of the new Q-value for the reaction $^{138}Ba(\alpha,t)^{139}La$, one may give the relative Q-value for the reaction $^{135}Ba(\alpha,t)^{136}La$ to be 14.418 $\pm$ 0.007 MeV.

The uncertainties in the masses of ^{139}La and ^{138}La are due to the uncertainty in the β^- end-point energy of ^{139}Ba decay, 5 keV. Also, the uncertainty in the mass of ^{135}La is drastically reduced from 120 keV to 11 keV. It is not known yet how the uncertainties have been reduced.

II.7 $(^3He,d)/(\alpha,t)$ Cross-section Ratios

The (α,t) reaction cross-sections, at 27 MeV, are an order of magnitude smaller than the $(^3He,d)$ cross-sections, at 24 MeV. Also the cross-sections are functions of the Q-values or the excitation energies. The interesting and useful feature of these reactions is that they favour different ℓ-values. The (α,t) reaction cross-section is largest for $\ell=5$ and 4, whereas the $(^3He,d)$ reaction is biased in populating $\ell=0$ and 2. This is due to the large difference between the angular momentum carried by the incoming α particle and the outgoing triton.

Exploiting the above properties of these proton transfer reactions, one is tempted to take the ratio of $(^3He,d)$ to (α,t) cross-sections, theoretically calculated by using the code DWUCK 4 (the optical model parameters are given in Tables II.2 and II.3) and generate a set of curves for $\ell=0$, 2, 4 and 5 by plotting the ratios of the cross-sections against the Q-values of the reactions. The optical model parameters for (α,t) reaction are given by Burke and Waddington, 1972. One spectrum of each reaction is required - the angles do not have to be the same in both the reactions. The $(^3He,d)$ and (α,t) reactions have to be normalized suitably before the ratios of the peak areas can be plotted against the appropriate excitation energy. This should, in principle, immediately indicate the ℓ-value for that state.

This method of obtaining ℓ-values would be fine where the proton is

Table II.4

The measured differences in Q-values

Reaction	Q-values (keV)		Q-value differences* (keV)			
	Gove & Wapstra	Wapstra & Bos	Gove & Wapstra	Wapstra & Bos	Islam	This Work
$^{138}Ba(\alpha,t)^{139}La$	-13614(14)	-13567(5)				
$^{137}Ba(\alpha,t)^{138}La$(a)	-13780(14)	-13734(5)	166	167	178(2)	---
$^{136}Ba(\alpha,t)^{137}La$(b)	-14190(syst)	-14294(syst)	576	727	713(3)	711(3)
$^{135}Ba(\alpha,t)^{136}La$(c)	-14360(70)	-14364(70)	746	797	---	851(4)
$^{134}Ba(\alpha,t)^{135}La$(d)	-14660(20)	-14822(11)	1046	1255	---	1268(3)

* These values represent the Q-value for $^{138}Ba(\alpha,t)^{139}La$ minus the Q-value for the stated reaction.

The sources from which the lanthanum masses were taken:

(a) Chidley (1958)

(b) Systematics

(c) Girgis (1959)

(d) Morinobu (1965)

Wapstra and Gove (1971)

Wapstra and Bos (1977) give the Q-values for (α,t) reactions on La isotopes in terms of the proton separation energy (Sp).

transferred to an even-even target to form an odd-A residual nucleus, because, the conservation of angular momentum and parity require a single ℓ-value contribution (Lu and Alford 1971). But complications arise when this technique is applied to odd-odd nuclei, such as ^{136}La, due to the fact that the same state can be populated by two ℓ-values via ℓ=0+2 or ℓ=2+4. The regions between ℓ=4 and ℓ=2 or ℓ=2 and ℓ=0 are highly non-linear, because, the cross-section is much larger for a lower ℓ then for a higher one. Therefore, a small admixture ℓ=2 in ℓ=4 would move the position of the point away from ℓ=4 curve. The same thing is true when there is ℓ=0 present in ℓ=2. Macphail and Summers-Gill (1976) were the first ones to apply this method successfully to the odd-odd nucleus ^{144}Pm.

Some nuclear physicists are reluctant to accept results obtained in this fashion. This technique would have to provide the accurate determination of admixtures of different ℓ-values and give unambiguous results to prove its validity, at least as far as the odd-odd nuclei are concerned. Nevertheless, this method is so simple and attractive that one is encouraged to explore the possibilities.

In the same experiment, ^{3}He and α beams were used on three barium isotopes, keeping all the experimental conditions the same. ^{134}Ba, ^{135}Ba and ^{138}Ba targets were used to obtain deuteron spectra at 45° and triton spectra at 50°. The choice of the angles was based on the following criteria:

(i) minimum interference from the light impurities,

(ii) the cross-section should not vary rapidly, and

(iii) the cross-section should not be small.

The ℓ-values of certain strongly populated states in ^{135}La and ^{139}La

are known from previous works. Six levels from ^{139}La and three from ^{135}La were chosen - not all the levels were strongly populated in both the reactions. The ratios of the cross-sections for these nine states of known ℓ-values were obtained and the family of curves which were generated by calculating the ratio of the theoretical cross-sections was best fitted to them. Unfortunately, the ground state of ^{139}La which is populated by ℓ_p=4 lies closer to the curve ℓ=5 than to ℓ=4. The ratios of the cross-sections for twenty-four states of ^{136}La were obtained and are plotted against their excitation energies in Fig. II.6. The ratio for the ^{139}La state at 1420 keV which is present in the ^{136}La spectra, did not coincide with the ratio which was measured separately. Therefore, all the ratios obtained with the ^{135}Ba target were multiplied by a factor ($\sim$0.77) to make those two points coincide.

Due to insufficient resolution in (^{3}He,d) spectrum, it was not possible to extract peak areas accurately. As a result, many ratios seem to lie in the region between ℓ=4 or ℓ=5. Obviously, they are either ℓ=4 or ℓ=5, because these ℓ-values cannot mix.

As mentioned earlier, the ground state of ^{136}La is populated by ℓ_p=2 and so are the first two excited states. The next triplet from 140 keV to 173 keV is populated by ℓ_p=4. Again, the 257 keV state is populated by ℓ_p=2. The next state 303 is believed to be populated by ℓ_p=4. From here on up until excitation of $\sim$800 keV all the states (10 in all) are populated by ℓ_p=2, 2+4 or 0+2, we have no way of being quantitative in our analysis from the ratio method. Then we have a state at 972 keV which is probably ℓ_p=4, also the next state (1006 keV) has ℓ_p=5. The cross-section of the next state (1028 keV) could not be obtained from the (^{3}He,d) spectrum, which is also populated by ℓ_p=5. The next two states are ℓ_p=5 at excitation

energies of 1076 and 1114 keV. For the rest of the states, not much can be said. Table III.2 lists all the ℓ_p values obtained either in this way or from the (^{3}He,d) angular distributions.

A remark should be made concerning the determination of the ℓ-values of the states which are populated by $\ell p=5$; it is evident that none of the methods, the angular distributions and the (^{3}He,d)/(α,t) cross-section ratios, give satisfactory results. This is mainly due to the fact that both techniques involve the (^{3}He,d) reaction which has considerably higher cross-sections for $\ell p=2$ or $\ell p=0$ than for $\ell p=5$. The higher level density beyond excitation energies of 1 MeV makes it difficult to obtain the cross-sections for the states populated by $\ell p=5$. Fortunately a very favourable situation exists in the (α,t) reaction where the cross-section for $\ell p=5$ is considerably higher than other ℓ transfers, which provides an opportunity to confirm the experimentally determined results and tentatively assign $\ell p=5$ values. One may refer to Fig. II.5.

Fig. II.6

The (^{3}He,d)/(α,t) cross-section ratios. The cross-sections for the deuteron spectrum are taken at 45° while those for the triton are measured at 50°. The solid curves are generated by using the DWBA calculations for a number of Q-values. They are renormalized as a family to fit the ratios of the nine states of known ℓ-values. Six of these states belong to ^{139}La and the remaining three to ^{135}La.

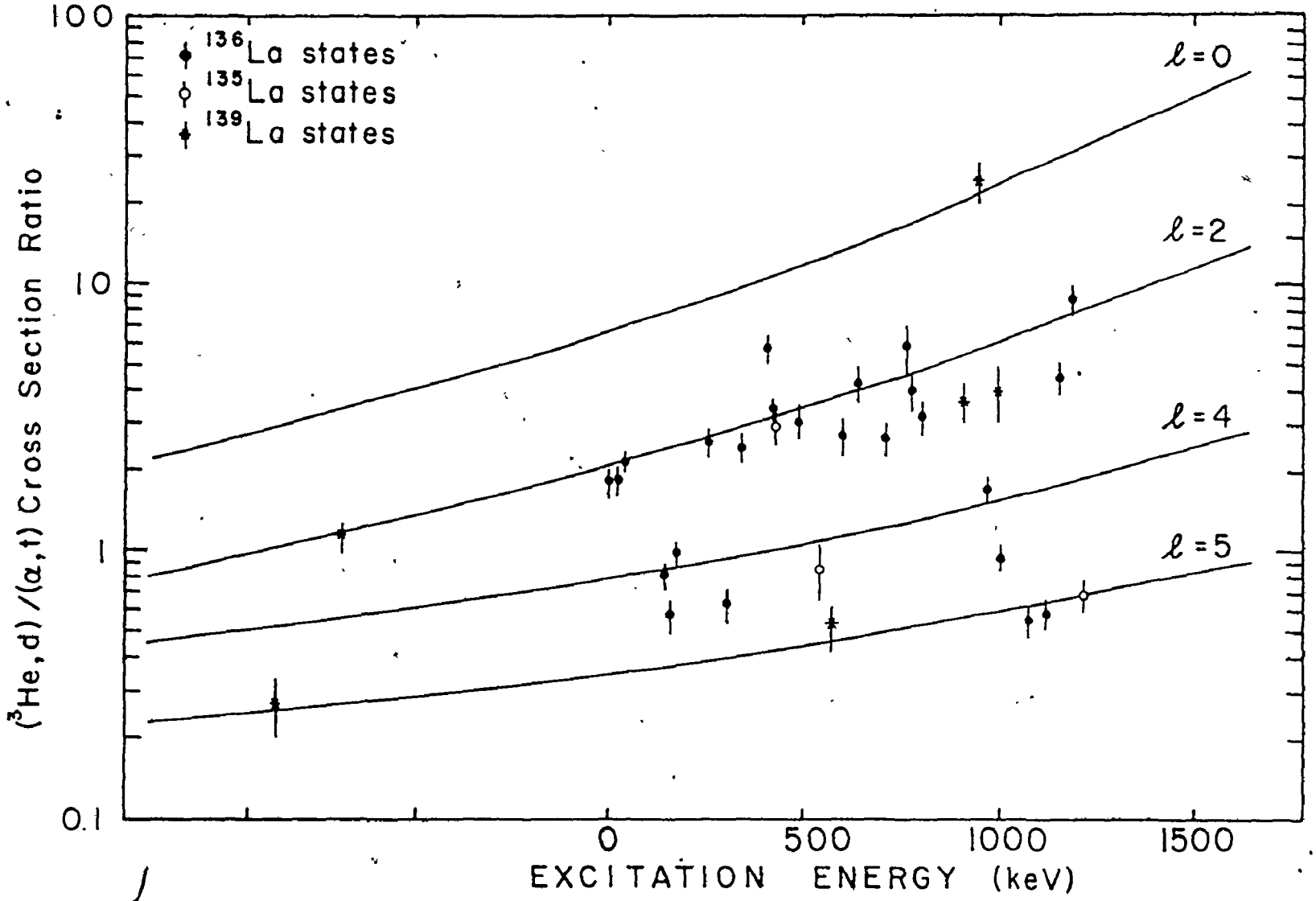
100
10
1
0.1
^{136}La states
^{135}La states
^{139}La states
ℓ=0
ℓ=2
ℓ=4
ℓ=5
$(^3He,d)/(\alpha,t)$ Cross Section Ratio
0
500
1000
1500
EXCITATION ENERGY (keV)

Chapter III

DISCUSSION AND INTERPRETATION OF THE RESULTS

Introduction

In the previous chapter we presented the experimental data and discussed the problems encountered in extracting conclusive information. The main problems were the high level density, the poor resolution and the background. However, ℓ-values have been determined for at least half of the levels. Both of the methods, the $(^3He,d)$ angular distributions and the $(^3He,d)/(\alpha,t)$ ratios, were useful in determining some of the ℓ_p-values, but they had their limitations. In the case of the angular distributions, it was very difficult to get the cross-sections for the same states at many angles. In the ratio method, the (α,t) cross-sections of the levels beyond $\sim$1200 keV fall very rapidly.

In this chapter we attempt to justify the tentative spin assignments for both the positive and negative parity states. This has been done on the basis of the amplitude factor $(2J_B+1)$. A comparison of ^{136}La with its neighbouring nuclei is also made, to show how much our expectations came true. In conclusion, the presence of an isomer is discussed and a few speculations are made.

III.1 Provisional Spin Assignments

III.1a The Low-lying Positive Parity States

It is expected that the simple shell model should adequately describe the low-lying levels. Although there should be 12 positive parity states only 8 of them would be populated in the proton transfer reaction in the absence of configuration mixing among the levels.

The ground state spin has been determined from β^+decay (Girgis et al., 1959) and it was found to be 1^+. On the basis of $(2J_B+1)$ the first and

second excited states appear to be 2^+ and 3^+ respectively. We think that the third, fourth and fifth excited states are populated by $\ell_p=4$. From their intensities in the (α,t) reaction, we tentatively assign 3^+, 5^+ and 2^+ to be their spins and parities, respectively.

There are two 4^+ states still to be accounted for. We know that the level at 257 keV is populated by $\ell_p=2$, therefore it is the most likely candidate for spin 4^+. Its strength is only 67% of what it should be leaving the remaining 33% to be accounted for. There is no single state that can carry all this left over strength. The other 4^+ state arising from $(\pi 1g_{7/2}, \nu\, 2d_{3/2}^{-1})$ configuration is at 304 keV. Again it carries little more than 40% of the strength - the state at 972 keV carries slightly less than 50% of the strength. We cannot say anything about the rest of the strength. This accounts for all the $J = 1^+, 2^+, 3^+, 4^+, 5^+$ arising from the configurations $(\pi 2d_{5/2}, \nu\, 2d_{3/2}^{-1})$ and $(\pi 1g_{7/2}, \nu 2d_{3/2}^{-1})$ and the configuration mixings involving $\nu 3s_{1/2}^{-1}$.

III.1b The Negative Parity States

We would expect to observe four strongly populated negative parity states formed by the coupling of a $h_{11/2}$ proton to the $d_{3/2}$ neutron hole giving $J=4^-$, 5^-, 6^- and 7^-. It is very difficult to assign the spins for such high spin states on the basis of the amplitude factor. Because their statistical weights are in the proportion of 9:11:13:15 which means that only a 15% change in intensity changes the spin.

The first negative parity state is encountered at an excitation energy of 1006 keV. There seems to be two more levels right after the first one at excitation energies of 1016 keV and 1028 keV. It is hard to judge whether there are actually two states or just one, but the program SPECTR is treating it as two. It makes more sense to treat them as one peak with

both the intensities added together. The next state has energy 1076 keV and it has the least intensity of the four. The last state is the strongest of all and its energy is 1114 keV.

Considering the strengths of the last two states one is tempted to assign the spins 4^- to the level with energy 1076 keV and 7^- to the state of excitation energy 1114 keV. If the adding of the intensities of the two levels, 1016 keV and 1028 keV, is correct then one might assign the spin to be 6^-. Then the 1006 keV state would have a 5^- spin.

These spin assignments have a more qualitative basis than quantitative one. All the spin assignments of the negative parity states are to be taken as suggestive. To be certain about the spins of these states, one requires better experimental data. Of course, the information from other experiments would also be valuable. See Table III.2.

III.2 ^{136}La and the Neighbouring Odd-A Nuclei

On comparing the structure of ^{136}La with its neighbouring odd-A La isotopes i.e. ^{135}La and ^{137}La, we can say that the low-lying states are more like ^{135}La and the negative parity proton states ($h_{11/2}$) are located at similar excitation energies as in the case of ^{137}La.

As expected, the ground state is populated by $\ell_p=2$ and so are the first and second excited states. ^{135}La has a state at $\sim$120 keV populated by $\ell_p=4$; in ^{136}La the strong $\ell_p=4$ states are found at excitation energies from $\sim$140 to $\sim$173 keV. One more interesting comparison shows that in ^{135}La, a state ($\sim$300 keV) has ambiguous spin $1/2^+$ or $3/2^+$ and, in ^{136}La a state ($\sim$333 keV) is believed to be populated by $\ell p=0+2$.

Also, the location of the proton $h_{11/2}$ state in ^{137}La is very similar to the first proton negative parity state, in fact within experimental

uncertainty they have the same energy.

From ^{135}Ba and ^{137}Ce, which have ($1h^{-1}_{11/2}$) neutron state at 268 keV and 254 keV, respectively, we guessed the location of the neutron hole states in ^{136}La to be around 260 keV. The existence of an isomer (discussed in the next sub-section) strongly suggests the presence of the negative parity neutron hole states in the very low-lying region. The comparison is summarized in Table III.1.

III.3 The Presence of an Isomer in ^{136}La

Now we discuss the possibility of the presence of a negative parity state in the deep low-lying energy region.

It has been mentioned in the introduction that γ-spectroscopy yields much better resolution which is highly desirable in the studies of odd-odd nuclei e.g. ^{136}La. Therefore, ^{136}Ba(p,nγ)^{136}La experiments have been carried out at various proton bombarding energies ranging from 7.5 to 4.2 MeV. Two Ge(Li) detectors, 50 c.c. and 14 c.c. were used to detect the γ's from ^{136}La in beam. These were singles experiments. It has been decided that coincidence experiments should be performed in the foreseeable future. An isomer of ^{136m}La has been reported by Gritsyna et al. (1966). They measured the half-life of the isomer to be ∿110 μsec and the energy of the isomeric state to be ∿170 keV which decays to the ground state through a level ∿100 keV.

The γ spectrum of ^{136}La shows two lines ∿2 keV apart; one at ∿96 keV and the other at ∿98 keV. The analysis of these (p,nγ) experiments has not been completed yet. Recently pulsed beam (p,nγ) experiments have been carried out and it has been ascertained that the 96 keV line is due to the isomer. In an old experiment with a steady beam of ^{11}B on natural Te target, Summers-Gill (1975) observed a line at ∿96 keV. Again in a subsequent

Table III.1

A comparison between ^{136}La and its neighbouring odd-A nuclei

Odd Proton						Odd Neutron	
	E_x keV			E_x keV		E_x keV	
Configuration	^{139}La	^{137}La	^{135}La	Configuration	^{136}La	Configuration	^{135}Ba	^{137}Ce
$\pi 2d_{5/2}$	166	10	0	$\pi 2d_{5/2}, \nu 2d_{3/2}^{-1}$	(0)	$\nu 2d_{3/2}^{-1}$	0	0
$\pi 1g_{7/2}$	0	0	120	$\pi 1g_{7/2}, \nu 2d_{3/2}^{-1}$	(140)			
				$\pi 2d_{5/2}, \nu 3s_{1/2}^{-1}$		$\nu 3s_{1/2}^{-1}$	221	160
				$\pi 2d_{5/2}, \nu 1h_{11/2}^{-1}$		$\nu 1h_{11/2}^{-1}$	268	254
$\pi 1h_{11/2}$	1418	1005	786	$\pi 1h_{11/2}, \nu 2d_{3/2}^{-1}$	(1006)			

The excitation energies of ^{136}La (shown in parentheses) are the energies of the first member of the particular configuration.

experiment with a pulsed beam of ^{11}B on ^{130}Te target, 10 μsec on and 10 μsec off, they observed a line at 96.3 keV.

It seems that there are two lines very close together both very intense in (p,nγ) reaction so they are transitions between low-lying levels but it is not necessary that they are decaying to the same state. One of them is the ∿96 keV line which is due to the above mentioned isomer. The half-life suggests it is an M2 transition which involves the decay of a negative parity state-presumably a $h^{-1}_{11/2}$ neutron state which would not be populated in the proton transfer reaction. However, the presence of the neutron hole state around such low excitation energies is still a mystery.

We think that the isomer is decaying from a level at ∿140 keV to the state at ∿45 keV. That would account for the ∿96 keV lines in γ-ray studies. But the observed 140 keV state is populated by $\ell_p=4$ and the parity is positive. We are looking for a high spin state of negative parity - we know where the proton negative parity states are - hence, it has to be a neutron hole negative parity state which lies around ∿140 keV that we cannot observe. But as mentioned earlier we would expect these states to be around 260 keV.

Another possibility seems to be plausible; there is a state very close to 140 keV which is fed by the isomer, which decays to the level at 45 keV.

Further coincidence experiments are required to solve this mystery.

Table III.2

Energies and cross-sections for levels observed in the $^{135}Ba(^{3}He,d)^{136}La$ and $^{135}Ba(\alpha,t)^{136}La$ reactions

Excitation Energy (keV)				Differential Cross-section (μb/sr)	
(^{3}He,d)	(α,t)	ℓ_p	J^π	25° (^{3}He,d)	50° (α,t)
0±1	0±1	2	1^+	61.0±3.2	22.2±1.0
22 1	22 1	2	$(2)^+$	94.4 4.0	34.1 1.0
45 2	45 1	2	$(3)^+$	151.0 5.0	48.7 1.2
140 4	140 1	4	$(3)^+$	23.7 2.0	21.6 1.1
159 4	159 1	(4)	(5^+)	27.1 2.1	33.7 1.5
173 4	173 2	4	$(2)^+$	13.0 1.5	16.4 1.3
	241 5				
257 2	257 1	2	$(4)^+$	172.0 5.4	44.6 1.2
303 3	304 2	4	$(4)^+$	11.6 1.4	11.1 0.5
323 3				10.9 1.4	
333 3	333 2	(0+2)		32.4 2.3	11.7 1.0
342 4	342 3			7.6 1.1	4.4 0.6
403 3	403 2	(2)		34.2 2.4	3.1 0.5
423 6	418 2[a]	(2)			
436 4	436 2	(4)		4.4 0.9	2.5 0.4
459 4				4.2 0.8	
484 4	484 2	(2)		22.3 2.0	3.9 0.4
500 5				9.8 1.3	
	543 3[a]				
594 6	594 3				1.8 0.4
608 4	605 3			7.9 1.2	
	617 3				2.3 0.4
626 3	629 3	(2)		31.4 2.3	6.2 0.6
646 3	643 3			7.5 1.1	1.2 0.4
704 6	704 3			10.8 1.4	2.1 0.4
716 6	716 3	(2)		10.3 1.3	1.3 0.4
726 6	726 3			2.8 0.7	1.1 0.4

Table III.2 (continued)

Excitation Energy (keV) (^{3}He,d)	Excitation Energy (keV) (α,t)	ℓ_p	J^π	Differential Cross-section (μb/sr) 25°(^{3}He,d)	Differential Cross-section (μb/sr) 50°(α,t)
	754±4	(2)			0.6±0.2
774±5	774±4	(2)		8.4±1.2	1.5±0.3
798 5	798 3	(2)		15.4 1.6	2.8 0.3
832 5	832 3			14.5 1.6	2.2 0.4
880 5				9.7 1.3	
907 6	906 3			17.7 1.7	2.0 0.4
966 5	972 2	4	$(4)^+$	38.5 2.5	12.8 2.0
988 8	999 3			25.5 2.1	10.1 2.1
1006 4	1006 2	5	$(5)^-$	56.5 3.1	36.6 2.8
	1016 2	(5)	$(6)^-$		18.0 2.4
1027 5	1028 2	5		34.6 2.4	19.9 2.4
1047 4	1042 4	(0)		34.8 2.4	6.0 3.0
1072 6	1076 3	(5)	(4^-)	47.6 2.8	32.2 1.5
1115 5	1114 3	(5)	(7^-)	61.2 3.3	43.2 2.0
1122 5				25.3 2.1	
1148 6	1155 4			32.2 2.3	5.2 1.2
1165 4	1165 4	(0+2)		38.7 2.5	2.2 0.5
1180 4	1180 4			47.1 2.8	3.7 0.4
1207 6	1200 5			23.6 2.0	1.3 0.3
1220 7				11.5 1.4	
1244 5	1247 6			11.5 1.4	1.4 0.3
1255 7	1257 6	(0+2)		18.7 1.8	2.2 0.4
1270 5				6.7 1.1	
1300 8				16.4 1.6	
1320 6				11.0 1.4	
1345 6				34.8 2.4	
1362 6				30.1 2.3	
1375 6				36.1 2.5	
1404 6				16.4 1.7	
1424 6				11.9 1.4	
1446 5				21.2 1.9	

Table III.2 (continued)

Excitation Energy (keV) (^{3}He,d)	(α,t)	ℓ_p	J^π	Differential Cross-section (μb/sr) 25° (^{3}He,d)	50° (α,t)
1458±5				25.2±2.1	
1471 5				10.6 1.3	
1500 5				20.7 1.9	
1557 5				32.6 2.3	
1570 4				43.0 2.7	
1593 5				15.8 1.6	
1644 6				25.5 2.1	
1686 6				26.7 2.1	
1707 3				31.7 2.3	
1745 4				22.0 1.9	

a) Most probably these levels are due to ^{135}La.

SUMMARY

The properties of some of the low-lying states of ^{136}La have been studied. It has been ascertained that simple shell model configurations can account for some of the experimentally investigated levels. At present, no other information is available concerning the structure of ^{136}La. The γ-ray studies are being carried out, which will complement this work and provide better understanding of the structure of ^{136}La.

The (^{3}He,d) reaction was utilized to determine some of the ℓ-values from the angular distribution analysis in terms of DWBA calculations. An alternate technique was utilized to obtain the ℓ-values from the ratios of (^{3}He,d) to (α,t) cross-sections. The applicability of this technique might prove to be useful for other odd-odd nuclei.

The forehand knowledge of the J^{π} of the ground state of ^{136}La and the determination of the ℓ-values from either one of the above mentioned methods provided the opportunity to tentatively assign spins to the first eight reasonably strongly populated states on the basis of 2J+1 rule. Also, the proton negative parity states were easily recognized from the (α,t) reaction.

The pulsed beam (p,nγ) and (^{11}B,5nγ) experiments have confirmed the existence of an isomeric state ($\sim$96 keV) due to an M2 transition involving a negative parity state due to a neutron hole configuration.

The (α,t) reactions on mixtures of barium isotope targets were useful in making accurate determination of differences of Q-values for the ^{134}Ba(α,t)^{135}La, ^{135}Ba(α,t)^{136}La and ^{135}Ba(α,t)^{137}La reactions in terms of the known Q-value of the reaction ^{138}Ba(α,t)^{139}La.

REFERENCES

Bartlett, J.H. 1932. Phys. Rev. 41, 370.

Bunting, R.L. 1975. Nuclear Data Sheets 15, 3.

Burke, D.G. and Balogh, J.M. 1975. Can. J. Phys. 53, 10.

Burke, D.G. and Waddington, J.C. 1972. Nucl. Phys. A193, 271.

Chidley, B.G., Katz, L. and Kowalski, S. 1958. Can. J. Phys. 36, 4.

Enge, H.A. 1958. Rev. Sci. Instr. 29, 885.

Elsasser, W. 1934. J. de Phys. et Rad. 5, 389.

Gamow, G. 1934. Zeits f. Physik 89, 572.

Ghoshal, S.N. 1950. Phys. Rev. 80, 939.

Girgis, R.D., Van Lieshout, R. 1959. Nucl. Phys. 12, 204.

Glaudemans, P.W.M., Brussaard, P.J. and Wildenthal, B.H. 1967. Nucl. Phys. A102, 593.

Gove, N.B. and Wapstra, A.H. 1972. Nucl. Data Tables 11, 127.

Green, I.M. and Moszkowski, S.A. 1965. Phys. Rev. 139, B790.

Gritsyna, V.T., Klyucharev, A.P. and Remaev, V.V. 1966. J. Nucl. Phys. (USSR) 3, 993.

Hussein, S.G. 1973. Ph.D. Thesis, McMaster University.

Ishimatsu, T., Ohmura, H., Awaya, T., Nakagawa, T., Orihara, H. and Yagi, K. 1969. J. Phys. Soc. Japan 27, 504.

Islam, A. 1975. Ph.D. Thesis, McMaster University.

Jensen, J.H.D., Haxel, O. and Suess, H.E. 1949. Phys. Rev. 75, 1766.

Kunz, P.D. 1969. Computer Code DWUCK, University of Colorado.

Lu, M.T. and Alford, W.P. 1971. Phys. Rev. C3, 1243.

Macphail, M.R. and Summers-Gill, R.G. 1976. Nucl. Phys. A263, 12.

Mayer, M.G. 1949. Phys. Rev. 75, 1969.

Morinobu, S., Hirose, T. and Hisatake, K. 1965. Nucl. Phys. 61, 613.

O'Neil, R.A. 1972. Ph.D. Thesis, McMaster University.

Pandya, S.P. 1956. Phys. Rev. 103, 956.

Racah, G. 1942. Phys. Rev. 62, 438.

Satchler, G.R. 1964. Nucl. Phys. 55, 1.

Satchler, G.R. 1965. "Lectures in Theoretical Physics", vol. VIII C, ed. Kunz, P.D., Lind, D.A. and Britton, W.T. University of Colorado Press, Boulder.

Spencer, J.E. and Enge, H.A. 1967. Nucl. Instr. and Methods 49, 181.

Summers-Gill, R.G. 1975. Private communication.

Wapstra, A.H. and Bos, K. 1977. Nucl. Data Tables 19, 3.

Wapstra, A.H. and Gove, N.B. 1971. Nucl. Data Tables 9, 265, 303.

Wildenthal, B.H. 1969. Phys. Rev. Lett. 22, 1118.

Wildenthal, B.H., Newman, E. and Auble, R.L. 1971. Phys. Rev. C3, 1199.